THE EFFECTS OF MUTUAL COUPLING BETWEEN ANTENNA ELEMENTS ON THE PERFORMANCE OF ADAPTIVE ARRAYS

A THESIS SUBMITTED TO
THE GRADUATE SCHOOL OF NATURAL AND APPLIED SCIENCES
OF
MIDDLE EAST TECHNICAL UNIVERSITY

BY

GÜNEY ÖZKAYA

IN PARTIAL FULFILMENT OF THE REQUIREMENTS FOR THE DEGREE OF
MASTER OF SCIENCE
IN
THE DEPARTMENT OF ELECTRICAL AND ELECTRONICS ENGINEERING

DECEMBER 2003

Approval of the Graduate School of Natural and Applied Sciences

Prof. Dr. Canan Özgen
Director

I certify that this thesis satisfies all the requirements as a thesis for the degree of Master of Science.

Prof. Dr. Mübeccel Demirekler
Head of Department

This is to certify that we have read this thesis and that in our opinion it is fully adequate, in scope and quality, as a thesis for the degree of Master of Science.

Y. Doç. Dr. Lale Alatan
Supervisor

Examining Committee Members

Prof. Dr. Altunkan Hızal _____

Prof. Dr. Ayhan Altıntaş _____

Assoc. Prof.Dr. Gülbin Dural _____

Assist. Prof. Dr. Lale Alatan _____

Assist. Prof. Dr. Özlem Aydın Çivi _____

ABSTRACT

THE EFFECTS OF MUTUAL COUPLING BETWEEN ANTENNA ELEMENTS ON THE PERFORMANCE OF ADAPTIVE ARRAYS

ÖZKAYA, Güney

M.S., Department of Electrical and Electronics Engineering
Supervisor : Assist. Prof. Dr. Lale ALATAN

December 2003, 54 pages

Array processing involves manipulation of signals induced on various antenna elements. In an adaptive array system, the radiation pattern is formed according to the signal environment by using signal processing techniques. Adaptive arrays improve the capacity of mobile communication systems by placing nulls in the direction of interfering sources and by directing independent beams toward various users.

Adaptive beamforming algorithms process signals induced on each array element that are assumed not to be affected by mutual coupling between the elements. The aim of this thesis is to investigate the effects of mutual coupling on the performance of various adaptive beamforming algorithms. The performance parameters such as signal to interference plus noise ratio and speed of convergence of the adaptive algorithms are studied and compared by both neglecting and considering the mutual coupling for the least mean squares,

recursive least squares, conjugate gradient and constant modulus algorithms. Finally, it is concluded that the effect of mutual coupling is major in the performance of blind algorithms rather than non-blind algorithms. The results are obtained by simulations carried out on MATLAB™.

Keywords: Adaptive Antenna Systems, Beamforming Algorithms, Mutual Coupling Effect.

ÖZ

ANTEN ELEMANLARI ARASINDAKİ KARŞILIKLI BAĞLAŞIMIN UYARLAMALI DİZİLERİN PERFORMANSI ÜZERİNDEKİ ETKİLERİ

ÖZKAYA, Güney

Yüksek Lisans, Elektrik ve Elektronik Mühendisliği Bölümü
Tez Yöneticisi: Y. Doç. Dr. Lale ALATAN
Aralık 2003, 54 pages

Dizi işlemesi, çeşitli anten elemanları üzerinde oluşan işaretlerin biçimlendirilmesini içerir. Bir uyarlamalı anten sisteminde ışıma örüntüsü, işaret işleme teknikleri kullanılarak mevcut işaret ortamına göre oluşturulur. Uyarlamalı diziler, istenmeyen yayınlar yönünde dalga sıfırları oluşturarak ve farklı kullanıcılar için bağımsız ışıma örüntüleri oluşturarak, hareketli haberleşme düzenlerinin kabiliyetini artırırlar.

Uyarlamalı hüzme oluşturan algoritmalar, her bir dizi elemanında oluşan ve elemanlar arasındaki karşılıklı bağlaşımdan etkilenmediği varsayılan işaretleri işlerler. Bu tezin amacı, karşılıklı bağlaşımın farklı hüzme oluşturma algoritmalarının başarımına olan etkisini incelemektir. İşaretin, gürültü ile girişimin toplamına oranı ve algoritmaların yaklaşım hızı gibi başarım göstergeleri, karşılıklı bağlaşımı göz önünde bulundurmadan ve bulundurarak, karelerin ortalamasının asgarisi, tekrarlamalı karelerin asgarisi, eşlenik gradyan yöntemi ve sabit büyüklük algoritmaları üzerinde incelenmiştir. Sonuçta, karşılıklı

bağlaşımın etkisinin, uyarlamalı kör algoritmalarda, uyarlamalı kör olmayan algoritmalara nazaran büyük olduğu sonucuna varılmıştır. Sonuçlar, MATLAB™ programında düzenlenen canlandırmalardan elde edilmiştir.

Anahtar Kelimeler: Uyarlamalı Anten Sistemleri, Hüzme Oluşturma Algoritmaları, Karşılıklı Bağlaşma Etkisi.

Gülşen'e

ACKNOWLEDGEMENTS

An ordinary sentence like, 'I would like to express my sincere appreciations to Assist. Prof. Dr. Lale Alatan for her guidance and support in this research' can not express my sincere thanks to my dear advisor. She is not only an advisor just giving advices but also a precious person one can rarely meet these days. She feels the responsibility of teaching like a primary school teacher with her degree of patience and has the attitude of questionning like Sokrates with her degree of academic suspicion. She is one of the suns of our young academic generation in this country who shines with science and humanism.

I would like to thank Assoc. Prof. Dr. Sencer Koç for letting me use his signal generation MATLAB subroutine.

I would also like to thank Aselsan A.Ş. for letting me to forward my precious time for this study.

Special thanks to Çağrı Acar for his documantary contributions.

My brother Güven Özkaya also deserves sincere thanks for his understanding as well as my parents.

My last thanks are to Gülşen for her great support, motivation, understanding, insistence and love.

TABLE OF CONTENTS

LIST OF FIGURES

LIST OF TABLES

TABLE

LIST OF ABBREVATIONS

AWGN : Additive White Gaussian Noise
BPSK : Bipolar Phase Shift Keying
CDMA : Code Division Multiple Access
CMA : Constant Modulus Algorithm
DOA : Direction of Arrival
DF : Direction Finding
E[.] : Expectation Operator
FDMA : Frequency Division Multiple Access
FFT : Fast Fourier Transform
GMSK : Gaussian Minimum Shift Keying
GTD : Geometrical Theory of Diffraction
INR : Interference to Noise Ratio
LMS : Least Mean Squares
MC : Mutual Coupling
MMSE : Minimum Mean Squared Error
MoM : Method of Moments
MSE : Mean Squared Error
NEC : Numerical Electromagnetics Code
QPSK : Quadrature Phase Shift Keying
RLS : Recursive Least Square
RMS : Root Mean Square
SNR : Signal to Noise Ratio
SINR : Signal to interference plus noise ratio
TDMA : Time Division Multiple Access

CHAPTER 1

INTRODUCTION

An array antenna consists of two or more antenna elements that are spatially arranged and electrically interconnected to produce a desired radiation pattern. The interconnection between elements is called the feed network. Feed network provides the appropriate excitation coefficients (both amplitude and phase) of each element that are synthesized according to the requirements of the desired radiation pattern.

In a conventional array, the excitation coefficients are fixed, whereas in an adaptive array the radiation and/or reception pattern are/is formed automatically according to the signal environment. These antenna systems are also referred to as "smart" arrays. What makes them smart is their signal processing capability. Different from a conventional array, adaptive arrays form patterns by adjusting the control weights (excitation coefficients) of each array element such that the desired signal power is maximized and the effect of the undesired signal components are minimized. In Chapter 2 of this thesis, the types of smart arrays are investigated. The properties of the switched beam systems and the adaptive systems are summarized and the terminology and signal model for adaptive arrays are presented.

Adaptive arrays have their roots in a number of different fields, including self phasing RF antenna arrays [1], [2], sidelobe cancellers [3], adaptive filters [4], [5], acoustic and sonar arrays, and seismic arrays. Various beamforming algorithms are developed up to date to adjust the array weights with different accuracy and

speed of convergence. Adaptive algorithms are grouped into two sections according to the utilization of a reference signal. The algorithm belongs to the non-blind group if it uses a reference signal. However, it is a blind algorithm if no reference signal is used. In Chapter 3, three non-blind adaptive algorithms; least mean squares (LMS) algorithm, recursive least squares (RLS) algorithm, conjugate gradient method (CGM) and one blind adaptive algorithm; constant modulus algorithms (CMA) are presented.

In adaptive array systems, the inputs of the beamforming algorithms are the measured signals at the antenna terminals. As the interelement spacing of the array gets smaller, the mutual coupling among the array elements becomes significant. Consequently the signal measured at the input of an antenna in an array environment turns out to be different than the signal measured at the input of an isolated antenna. Due to this variation in the measured signals, caused by the mutual coupling between the antenna elements, the performance of adaptive beamforming algorithms may be affected. [11], [17], [18] are examples of the studies that investigate the effects of mutual coupling.

Adve and Sarkar used the method of moments (MoM) to evaluate the mutual coupling between the elements of a given array. The MoM admittance matrix is then used to eliminate the effects of mutual coupling in measured signals [17].

B. Friedlander and A. J. Weiss developed an eigenstructure based method for direction finding (DF) in the presence of mutual coupling, gain and phase uncertainities which provides estimates of direction of arrival (DoA) of all the radiating sources as well as calibration of gain, phase of each sensor and mutual coupling in the receiving array [18].

The mutual coupling effect among the array elements and the diffraction effect caused by the conducting plate were taken into account in the calculation by a hybrid method of moment method (MoM) and geometrical theory of diffraction (GTD) in [11]. Simulations showed that the CMA adaptive array performs

differently when the mutual coupling and the diffraction effects are taken into account.

Steyskal and Herd developed a mutual coupling compensation method [14] to eliminate the performance reduction in the presence of considerable mutual coupling. In this method, the mutual coupling matrix for arrays of single mode elements is used to update the measured signals.

Chapter 4 presents the method applied to incorporate the effect of mutual coupling in adaptive algorithms.

In Chapter 5, simulation results carried on MATLAB^{TM} are given. Performance of adaptive algorithms using measured data with mutual coupling are compared with the results obtained if no mutual coupling were present. The effects of mutual coupling in different adaptive algorithms are investigated for different communication scenarios. Finally a conclusion is provided in Chapter 6.

CHAPTER 2

SMART ANTENNA SYSTEMS

Several terms are referred to the smart antenna system technology according to the applications. Those are intelligent antenna, phased arrays, spatial division multiple access (SDMA), spatial processing, digital beamforming, adaptive antenna systems and others. Smart antenna systems are categorized, as either switched beam or adaptive antenna arrays. A switched beam system utilizes a finite number of fixed, predefined patterns, an adaptive system utilizes an infinite number of patterns that are adjusted in real time.

Smart antennas offer solutions to various types of performance degradation problems of a communication system by adaptively forming a beam pattern. The advantages of a smart antenna system can be better understood when the three major factors that affect the performance of a communication system are investigated. The first one is the multipath fading, which is caused by received signals arriving through multiple paths. Received signal amplitude and phase vary due to those additive signals. Antenna look direction, location and polarization change the degree of effect of multipath fading. Second is the difference in propagation delays among the multiple paths, namely delay spread. Intersymbol interference arise when the delay spread exceeds above a certain value of symbol duration. The third is the co-channel interference. Cellular systems divide the usable frequency channels into sets and use each channel for one cell with frequency reuse. As the number of channel sets decreases i.e. as the capacity of each cell increase, the co-channel interference occur [6]. Therefore, in the

transmitting mode, co-channel interference can be reduced by directing the main beam in the direction of the desired signal, and putting nulls in the directions of undesired receivers. Similarly, in the receiving mode, co-channel interference can be reduced by forming a reception pattern so that the desired signal source power is maximized and the directional location of the undesired signal sources are cancelled.

Both switched beam and adaptive systems attempt to maximize gain according to the location of the user. However, only the adaptive system provides an optimization of the desired signal reception while at the same time identifying, tracking, and minimizing undesired signals. The adaptive systems are able to form a beam pattern in certain directions and automatically steer a null position in spatial domain. This capability is the principal advantage of adaptive techniques. In addition to the automatic interference nulling, they can also be designed to eliminate multipath signals.

In the following sections, the properties of the switched beam systems and the adaptive systems will be summarized.

2.1 SWITCHED BEAM SYSTEMS

Switched beam systems form predetermined beams, sectors, in certain directions with increased gain. The coverage pattern of a switched beam system is the combination of these predetermined beams as shown in Figure 2.1. One of those beams is chosen to send/receive signal to/from the desired target, the user. When the user moves around, the operating beam is switched to the one that receives the maximum amount of power.

In the current cellular sectorization method, a typical sectorized cell site has three 120 degree macro-sectors. With the switched beam approach, macro-sectors are further more subdivided into several micro-sectors. Each micro-sector contains a predetermined fixed beam pattern with the highest sensitivity in the center of the main beam. When the mobile user enters a particular macro-sector, the switched

beam system selects from several choices of the micro-sectors the one that contains the strongest signal during operation. Throughout the communication, the system monitors signal strength and switches to other micro-sectors when needed.

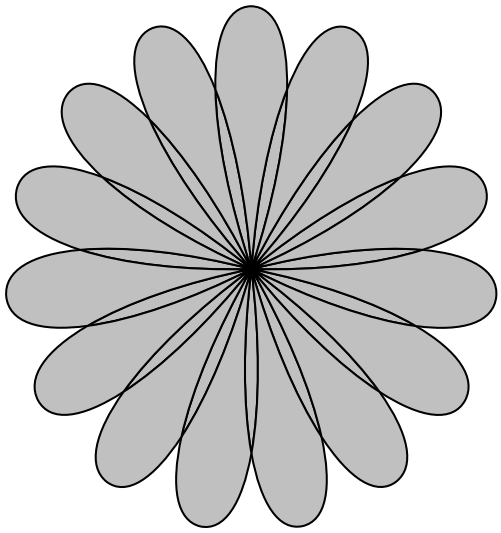

Figure 2.1 Coverage Pattern of a Switched Beam System (sectors)

There are, however, some restrictions to the switched beam systems. As the beams are predetermined, the signal strength varies while the user moves through the sector. When a user moves toward the edges of a sector beam, the signal strength can degrade rapidly before the user is switched to another micro-sector. Another limitation occurs when identifying the desired signal. A switched beam system cannot distinguish between a desired signal from interfering ones. In some cases, interfering signal can be enhanced far more than the desired signal which is a problem of the quality degradation.

2.2 ADAPTIVE ANTENNA SYSTEMS

The adaptive antenna approach represents the most advanced smart antenna technology up to date. An adaptive antenna system continuously updates its beam pattern based on changes in both the desired and interfering signal locations. Its

principal ability is to track users with main lobes and interferers with nulls. There are neither micro-sectors nor predefined patterns. As seen in Figure 2.2, the main beam is directed toward the desired user and a null is formed in the direction of an undesired user. This effect can be better explained by making an analogy to the human hearing system as discussed in [6]. When one person listens to another, the brain of the listener collects the sound in both ears, combines it to hear better, and determines the direction from which the speaker is talking. If the speaker is moving, the listener, even if her eyes are closed, can continue to update the angular position based solely on what she hears. The listener also has the ability to tune out unwanted noise, interference, and focus on the conversation at hand.

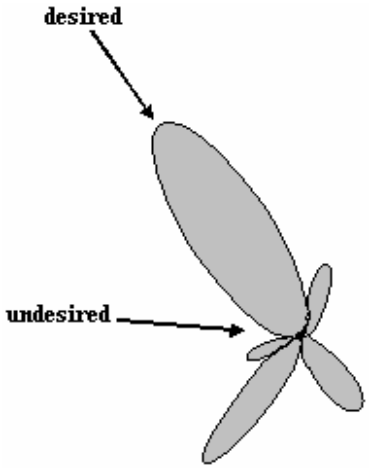

Figure 2.2 Pattern of an Adaptive Array System

The adaptive approach is different from the switched type with its ability to continuously change the radiation pattern with respect to both main beams and nulls. As interfering signals move throughout the sector, the switched beam pattern is not changed. It only responds to movements in the signal of interest. When an interfering signal begins to approach the signal of interest, the communication quality with the desired signal will degrade accordingly. Adaptive antenna technology can dynamically form signal patterns to optimize the performance of the communication system.

2.3 ADAPTIVE ANTENNA SYSTEM DESCRIPTION

There are many beamforming schemes utilized in adaptive array systems such as narrow-band beamformer, delay and sum beamformer, broad-band beamformer, beam-space beamformer, optimal beamformer etc. [7]. For various types of communication requirements, one of these schemes is utilized in an adaptive array system.

In this thesis a narrow-band beamformer will be investigated. To construct the notation and the terminology, consider an equispaced array of L isotropic identical antenna elements aligned linearly in free space. The array lies in the far field of M uncorrelated sources with carrier frequency f_o one of which is shown in Figure 2.3. Θ_i is the angle measured from the normal of the array axis denoting the direction of the i^{th} signal source. The figure depicts the plane for azimuth angle $\phi_i = \pi / 2$.

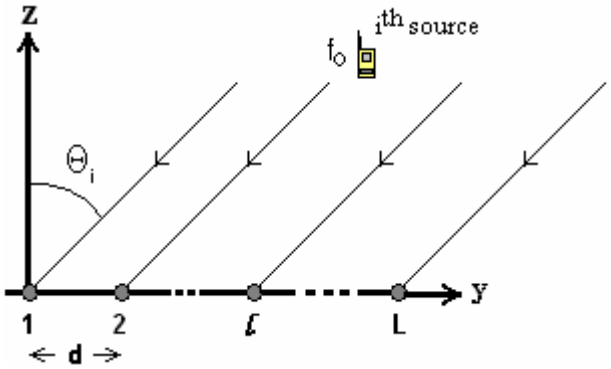

Figure 2.3 L isotropic elements aligned in free space

The signal wavefront arrives to the first element situated at the origin, τ_l seconds later than the ℓ^{th} element. This retardation is given by

$$\tau_l(\Theta i) = (d/c)(l-1)\sin\Theta_i \qquad (2.1)$$

where d is the interelement distance and c is the speed of light. The signal induced on the element at the origin due to the i^{th} source is normally expressed in complex

notation as

$$m_i(t)e^{j2\pi f_0 t} \tag{2.2}$$

with $m_i(t)$ denoting the complex modulating function. The structure of the modulating function reflects the particular modulation used in a communication system. Assuming that the wavefront on the l^{th} element arrives τ_l (Θi) seconds before it arrives at the first element, the signal induced on the l^{th} element due to the i^{th} source can be expressed as

$$m_i(t)e^{j2\pi f_0(t-\tau_l(\Theta_i))} \tag{2.3}$$

The expression is based upon the narrow-band assumption for array signal processing, which assumes that the bandwidth of the signal is narrow and the array dimensions are small such that the modulating function stays almost constant during τ_l (Θi) seconds [7].

Let x_l denote the total signal induced on the l^{th} element due to all directional sources and background noise. Then it is given by

$$x_l = \sum_{i=1}^{M} m_i(t)e^{j2\pi f_0(t+\tau_l(\Phi_i,\Theta_i))} + n_l(t) \tag{2.4}$$

where n_l (t) is a random noise component on the l^{th} element, which includes background noise and electronic noise generated in the l^{th} channel. It is assumed to be temporally white with zero mean and variance equal to σ_n^2. It should be noted that this expression is valid only when the mutual coupling is neglected.

Consider a narrow-band beam former, as shown in Figure 2.4, where the signals from each element are multiplied by a complex weight and summed to form the array output.

The figure does not show components such as preamplifiers, bandpass filters, and so on. It follows from the figure that an expression for the array output is given by

$$y(t) = \sum_{l=1}^{L} \underline{w}_l^* \underline{x}_l(t) \tag{2.5}$$

When the weights of the beamformer and time samples of signals induced on all elements are expressed in vector form, the output of the beamformer becomes

$$y(t) = \underline{w}^H \underline{x}(t) \tag{2.6}$$

where

$$\underline{w} = [w_1, w_2, \ldots, w_L]^T \tag{2.7}$$

$$\underline{x}(t) = [x_1(t), x_2(t), \ldots, x_L(t)]^T \tag{2.8}$$

where superscripts T and H, respectively, denote the transpose and complex conjugate transpose of a vector or matrix. Throughout this thesis, $\underline{w}$ and $\underline{x}(t)$ are referred to as the array weight vector and the array signal vector, respectively.

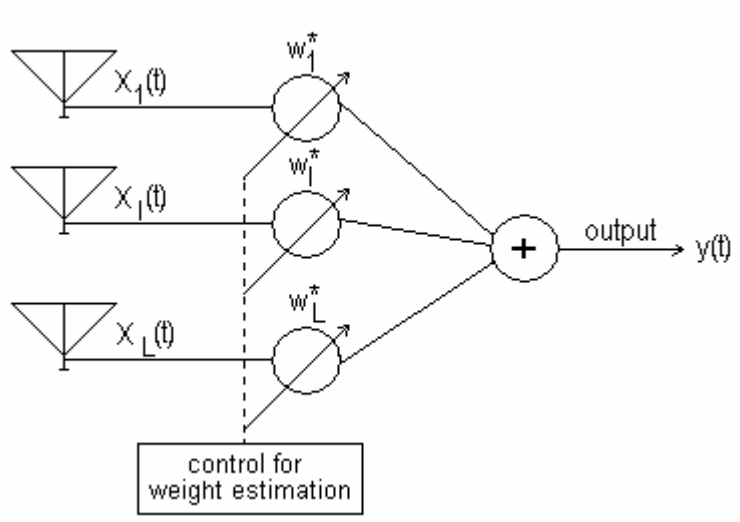

Figure 2.4 Narrow-band beam-former structure

If the components of $\underline{x}(t)$ can be modeled as zero mean stationary processes, then for a given $\underline{w}$, the mean output power of the processor is given by

$$P(\underline{w}) = E[y(t)\, y(t)^H] = \underline{w}^H \mathbf{R}\, \underline{w} \tag{2.9}$$

where E[.] denotes the expectation operator and **R** is the array correlation matrix

defined by

$$\mathbf{R} = E[\underline{x}(t)\,\underline{x}(t)^H] \tag{2.10}$$

Elements of this matrix denote the correlation between array elements. For example, R_{ij} denotes the correlation between the i^{th} and the j^{th} element of the array.

There are many schemes to select the weights of the beam former depicted in Figure 2.4, each with its own characteristics and limitations. Some of these are discussed in the following chapter.

CHAPTER 3

ADAPTIVE BEAMFORMING ALGORITHMS

There are many weight estimation algorithms deployed for beamforming in adaptive array systems. They are grouped into two as blind and non-blind adaptive algorithms. Blind adaptive algorithms do not require a reference signal input. But, on the other hand, non-blind adaptive algorithms need a reference signal input to estimate weights. A simplified functional block diagram of blind adaptive algorithms is shown in Figure 2.4. No input reference signal is used to estimate the weights in the control block. However, in a non-blind adaptive algorithm, a reference signal should be used as a priori knowledge to update weights. An error signal is utilized for estimation of weights in feedback loop as seen in Figure 3.1.

Depending upon the application, the reference signal may be generated in a number of ways. In digital mobile communications, a synchronization signal may be used for initial weight estimation, followed by the use of detected signal as a reference signal [7]. In systems using a TDMA scheme, a sequence that is user specific may be a part of every frame for this purpose [8]. In systems using CDMA scheme, pseudo noise codes (PNC) with different generators for the individual users are used [11]. In other situations, the use of an antenna for this purpose has been examined to show the suitability to provide a reference signal [9]

3.1 NON-BLIND ADAPTIVE ALGORITHMS

Non-blind adaptive algorithms generate an error signal which is the difference between the array output and an available reference signal $\underline{r(t)}$, expressed as

$$e(t) = \underline{w}^H \underline{x}(t) - r(t) \tag{3.1}$$

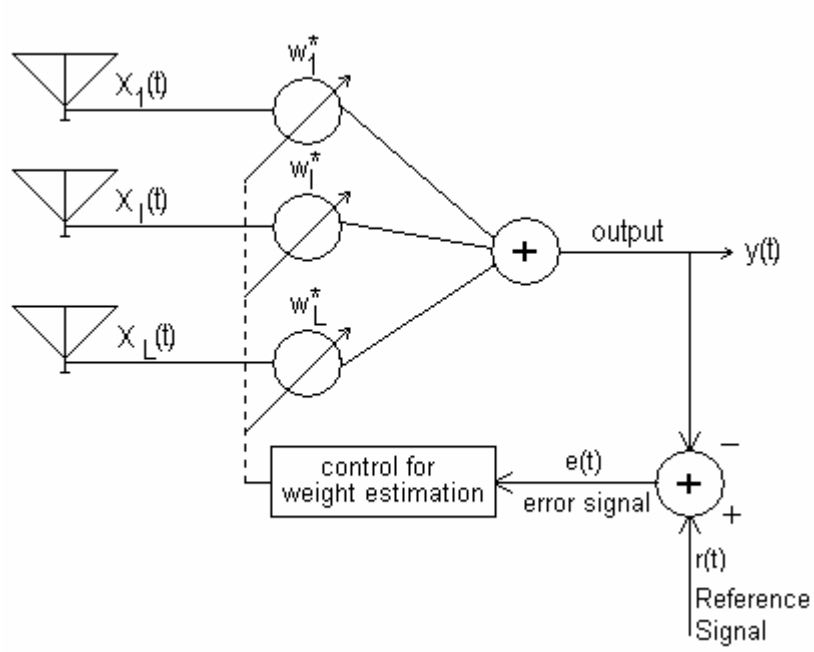

Figure 3.1 Functional block diagram of non-blind adaptive algorithms

Error information is an indication of the distance from the correct solution, therefore it is a mean to control the weights of array elements. Most of the adaptive algorithms are based on the principle that the weight vector should be optimized such that the mean square of the error (MSE) is minimized. The MSE is given by

$$\begin{aligned} \text{MSE} &= \text{E}[|e(t)|^2] \\ &= \text{E}[|r(t)|^2] + \underline{w}^H \mathbf{R} \underline{w} - 2\underline{w}^H \underline{z} \end{aligned} \tag{3.2}$$

where

$$\underline{z} = \text{E}[|\underline{x}(t)\, r^*(t)|] \tag{3.3}$$

is the correlation between the complex conjugate of the reference signal and

the array signals vector $\underline{x}(t)$ and **R** is the array correlation matrix defined by equation 2.9. The MSE is a quadratic function of $\underline{w}$ and is minimized by setting its gradient with respect to $\underline{w}$ equal to zero, yielding the Wiener-Hopf equation for the optimal weight vector

$$\underline{w}_{MMSE} = \mathbf{R}^{-1}\underline{z} \tag{3.4}$$

In the application of adaptive arrays, the exact evaluation of the **R** matrix and the $\underline{z}$ vector are not possible, since only a finite number of samples of $\underline{x}$ vector are available at time steps $n\Delta T$. In that case, the best approximation for the expectation operator appearing in the optimal solution (in **R** and $\underline{z}$) is the ensemble average of N time samples. When the expected value is replaced with the average value of N snapshots, the method is called Sample Matrix Inversion (SMI). However SMI is not an efficient method for a real-time system since one needs to wait for N time steps to update the weight vector. Therefore iterative methods that update the weight vector at each time step are preferred in most of the applications. Since the least mean squares (LMS), the recursive least squares (RLS) and the conjugate gradient method (CGM) are the most commonly used iterative methods, they are chosen to be the algorithms studied in this thesis. Details of these algorithms will be summarized in the following sections.

3.1.1 Least Mean Squares Algorithm

The determination of the optimal weights in an adaptive array is equivalent to the solution of an optimization problem in which the MSE is minimized. The optimization problem can be expressed as

$$\min_{\underline{w}} MSE(\underline{w}) = \underline{w}^H \mathbf{R}\underline{w} - 2\underline{w}^H \underline{z} \tag{3.5}$$

In LMS algorithm, the steepest descent method (SDM) is used for the solution of this optimization problem. SDM is an iterative algorithm and at each iteration, the solution vector (weight vector for this case) is updated in the direction of steepest descent which is the opposite direction to the gradient of the cost function. The iterations start with an initial value of weight vector, $\underline{w}(0)$, chosen

arbitrarily and every new selection of weight vector, $\underline{w}(n+1)$, can be written in the form

$$\underline{w}(n+1) = \underline{w}(n) - \mu(n)\, \underline{g}(\underline{w}(n)) \tag{3.6}$$

where μ is the step size and $\underline{g}(\underline{w}(n))$ is the gradient of the cost function.

The convergence pattern of the iterations are shown in Figure 3.2 for a two dimensional problem. Each gradient is orthogonal to the previous gradient. Therefore the convergence follows a zigzag path.

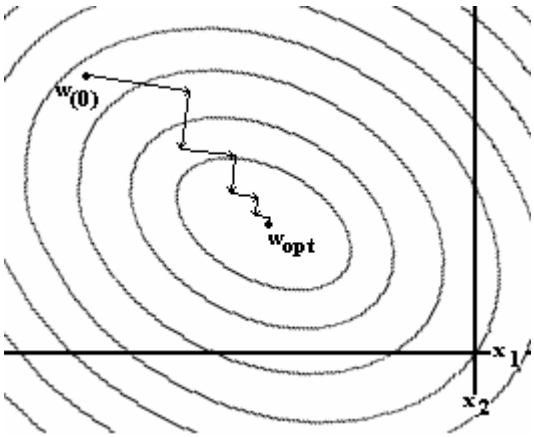

Figure 3.2 Convergence in the method of steepest descent

If it were possible to make exact measurements of the gradient vector at each iteration, and if the step size parameter μ were suitably chosen, then $\underline{w}(n)$ would converge to $\underline{w}_{opt}$. But, in reality, that is not the case. The gradient vector should be estimated from the available data. LMS algorithm uses an estimate of the gradient by replacing $\mathbf{R}$ and $\underline{z}$ with their instantaneous noisy estimates available at the n^{th} iteration, leading to

$$\begin{aligned} \underline{g}(n) &= 2\mathbf{R}\underline{w}(n) - 2\underline{z} \\ \underline{g}(n) &= 2\underline{x}(n)\underline{x}^{H}(n)\underline{w}(n) - 2\underline{x}(n)r^{*}(n) \\ &= 2\underline{x}(n)e^{*}(n) \end{aligned} \tag{3.7}$$

where $\underline{g}(n)$ represents the estimated gradient and $e^{*}(n)$ is the complex conjugate of the error between the reference signal and the array output, as given in equation

(3.1). It is clear that selection of the step size plays an important role on the convergence of the LMS algorithm. Two different approaches are widely used for the selection of the step size.

As discussed in literature [7], the first selection approach is based on the properties of the **R** matrix. As the sum of all eigenvalues of **R** equals its trace, the sum of its diagonal elements, one may select the gradient step size μ in terms of measurable quantities using $\mu<1/T_r(\mathbf{R})$, with $T_r(\mathbf{R})$ denoting the trace of **R**. It should be noted that each diagonal element of **R** is equal to the average power measured on the corresponding element of the array. Thus, for an array of identical elements, the trace of **R** equals the power measured on any element times the number of elements in the array.

In the second approach, the value of step size is chosen such that it minimizes the cost function. That is

$$\frac{\partial MSE(\underline{w}(n)-\mu\underline{g}(n))}{\partial\mu}=0 \tag{3.8}$$

The solution of equation (3.8) results in the following step size selection

$$\mu(n)=\frac{\underline{g}^T(n)\underline{g}(n)}{\underline{g}^T(n)\mathbf{R}\underline{g}(n)} \tag{3.9}$$

Note that the approach summarized above is applicable only for quadratic cost functions which is the case for adaptive array problems.

3.1.2 Recursive Least Squares Algorithm

As mentioned in the previous section, the convergence of the LMS algorithm depends upon the eigenvalues of **R**. Selection of μ, which minimizes the cost function, is very important for the convergence speed of the algorithm. A small error that can be done when choosing the step size may increase the time that the algorithm converges to the optimum solution. This problem is solved in an RLS

algorithm [7] by replacing the step size with the inverse of **R** matrix, producing the weight update equation

$$\underline{w}(n+1) = \underline{w}(n) - \mathbf{R}(n)^{-1}\underline{g}(n) \tag{3.10}$$

where **R**(n) is a linear combination of the **R** matrix of the previous iteration and the noisy estimate of **R** at the present iteration. It is given by

$$\mathbf{R}(n) = \delta_0 \mathbf{R}(n-1) + \underline{x}(n)\underline{x}^H(n) \tag{3.11}$$

where δ_0 is the forgetting factor which is a measure of memory for the algorithm. Relating each new **R** matrix to the previous, decreases the effect of the probability of the error done at one snap shot to the final estimation. For a special case, δ_0 equals 1 represents infinite memory which emphasizes old samples and δ_0 equals 0 represents a memoryless system.

To compute the optimal weight vector, the inverse of the correlation matrix should be determined. To avoid such a time consuming operation, the RLS algorithm updates the required inverse of **R** using the inverse of **R** calculated in the previous iteration and the present samples. When the inverse of **R** is computed by using the Matrix Inversion Lemma [7] the following expression is obtained:

$$\mathbf{R}^{-1}(n) = \frac{1}{\delta_0}\left[\mathbf{R}^{-1}(n-1) - \frac{\mathbf{R}^{-1}(n-1)\underline{x}(n)\underline{x}^H(n)\mathbf{R}^{-1}(n-1)}{\delta_0 + \underline{x}^H(n)\mathbf{R}^{-1}(n-1)\underline{x}(n)}\right] \tag{3.12}$$

The matrix is initialized as

$$\mathbf{R}^{-1}(0) = \frac{1}{\varepsilon_0} I, \varepsilon_0 > 0 \tag{3.13}$$

A discussion on the selection of ε_0 and its effects on the performance of the algorithm can be found in [15].

3.1.3 Method of Conjugate Gradients

The MSE, which is the cost function for the adaptive array problem, is a quadratic function. Therefore, minimization of the cost function is equivalent to the solution of a linear system of equation, which is represented mathematically as follows:

$$\min_{\underline{w}} \underline{w}^H \mathbf{R}\underline{w} - 2\underline{w}^H \underline{z} \equiv Solving \ \mathbf{R}\underline{w} = \underline{z} \tag{3.14}$$

when the expected values are replaced with their noisy estimates at the n^{th} time samples, the linear system of equations take the following form

$$\underline{x}(n)\underline{x}^{\mathrm{H}}(n)\underline{w} = \underline{x}(n)r^*(n) \tag{3.15}$$

Let **A** denote $\underline{x}(n)\underline{x}^{\mathrm{H}}(n)$ matrix, and $\underline{b}$ denote $\underline{x}(n)r^*(n)$ vector. Then the linear system of equations becomes $\mathbf{A}\underline{w}=\underline{b}$. The conjugate gradient method can be used to efficiently solve this linear system of equations.

Similar to the SDM, CGM is a directional search algorithm where at each iteration the solution vector is updated as follows

$$\underline{w}(n+1) = \underline{w}(n) + \mu(n)\underline{d}(n) \tag{3.16}$$

where $\underline{d}(n)$ is the search direction and $\mu(n)$ is the step size. In CGM, the choices of the search direction and the step size are different from the choices in the SDM. In CGM, the iterations start with the same search direction as the SDM, which is the opposite direction to the gradient of the quadratic cost function given as

$$\underline{d}(0) = -\underline{g}(0) = \underline{b} - \mathbf{A}\underline{w}(0) \tag{3.17}$$

To find the step size and the new search direction, the SDM should be revisited and its draw backs should be recognized.

The method of steepest descent often travels through the same directions as earlier iterations as shown in Figure 3.2. But if the right amount of step size and the

right search direction are computed, the iterations would end in two steps as illustrated in Figure 3.3, for a two dimensional problem. First step is from the starting point $\underline{w}(0)$ to $\underline{w}(1)$ in the direction of steepest descent, and the second is from the $\underline{w}(1)$ to $\underline{w}_{\text{opt}}$.

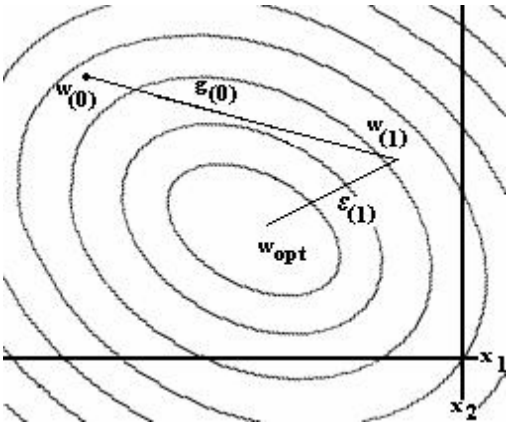

Figure 3.3 Convergence in the method of conjugate gradients

Note that, in order to reach the optimum solution in two steps, the new search direction should be in the same direction as the error vector which is defined as

$$\underline{\varepsilon}(n) = \underline{w}(n) - \underline{w}_{opt} \tag{3.18}$$

The gradient vector is related to the error vector as follows

$$\mathbf{A}\underline{\varepsilon}(n) = \mathbf{A}\underline{w}(n) - \mathbf{A}w_{opt} = \mathbf{A}\underline{w}(n) - \underline{b} = \underline{g}(n) \tag{3.19}$$

By imposing the condition that the cost function should be minimized for the optimum step size, the following important relation that forms the basis of CGM is obtained

$$\underline{d}^{H}(0)\underline{g}(1) = \underline{d}^{H}(0)\mathbf{A}\underline{\varepsilon}(1) = 0 \tag{3.20}$$

The condition given in equation (3.20) implies that the direction vector of the previous iteration and the error vector of the current iteration are **A** orthogonal. Recalling the fact that the next direction vector should be parallel to the error

vector, the condition given in equation (3.20) can be generalized such that the successive direction vectors should be **A** orthogonal to each other. To generate a set of **A** orthogonal vectors Gram-Schmidt orthogonalization process can be used. In the beginning of this process, a set of linearly independent vectors are chosen. Next, the direction vectors are computed by the following relation

$$\underline{d}(n+1) = -\underline{g}(n+1) + \beta(n)\underline{d}(n) \tag{3.21}$$

where the scalar parameter β(n), is found through the use of the **A** orthogonality property of the direction vectors.

$$\underline{d}^{H}(n)\mathbf{A}\underline{d}(n+1) = -\underline{d}^{H}(n)\mathbf{A}\underline{g}(n+1) + \beta(n)\underline{d}^{H}(n)\mathbf{A}\underline{d}(n) = 0 \tag{3.22}$$

$$\beta(n) = \frac{\underline{d}^{H}(n)\mathbf{A}\underline{g}(n+1)}{\underline{d}^{H}(n)\mathbf{A}\underline{d}(n)} \tag{3.23}$$

In CGM, the initial direction vector is chosen to be the negative of the gradient vector. By using the condition given in equation (3.20) the optimum step size is expressed as:

$$\mu(n) = -\frac{\underline{d}^{H}(n)\underline{g}(n)}{\underline{d}^{H}(n)\mathbf{A}\underline{d}(n)} \tag{3.24}$$

By combining equations (3.21) and (3.23) the weights are updated using equation (3.16).

3.2 BLIND ADAPTIVE ALGORITHMS

Unlike non-blind adaptive algorithms, blind adaptive algorithms do not utilize a reference signal information. Thus they are open-loop systems. The most popular one of the blind adaptive algorithms is the constant modulus algorithm (CMA).

3.2.1 Constant Modulus Algorithm

Constant modulus algorithm is a gradient-based algorithm that eliminates the amplitude fluctuations of the array output due to the existence of the interferences. Without those fluctuations, the array output has a constant modulus. CMA is useful for eliminating correlated arrivals and is effective for constant modulated envelope signals such as Bipolar Phase Shift Keying (BPSK), Gaussian Minimum Shift Keying (GMSK) and Quadrature Phase Shift Keying (QPSK), which are used in digital communications. For CMA(p,q), the algorithm updates the weights by minimizing the cost function

$$J(n) = \frac{1}{2} E\left[\left(|y(n)|^p - y_0^p \right)^q \right] \tag{3.25}$$

where p and q are positive integers, y_0 is the amplitude of the array output in the absence of interference and y(n) is the array output after the n^{th} iteration. By applying the steepest descent method, the beamformer weight vector is updated as

$$\underline{w}(n+1) = \underline{w}(n) - \mu g(n) \tag{3.26}$$

The expected value from the finite data of a series can not be obtained exactly. Thus, the expectation symbol must be removed from the updated equation. An average of a finite number of data samples, L, is used to replace the expected value. Then, for CMA(2,2) the cost function for p=q=2 becomes [11].

$$J(n) = \frac{1}{L} \sum_{i=k}^{k+L-1} \left[\left| |y_i(k)|^2 - y_0^2 \right|^2 \right] \tag{3.27}$$

where L is the number of data used for averaging and y(n) is

$$y(n) = \underline{w}^H(n)\underline{x}(n) \tag{3.28}$$

Similar to the LMS algorithm discussed previously, it uses an estimate of the gradient by replacing the true gradient with an average of L samples given by

$$g(n) = 2\varepsilon(n)\underline{x}(n+1) \tag{3.29}$$

$$\underline{g}(n) = 2(|y(n)|^2 - y_0^2)y(n)\underline{x}(n+1) \tag{3.30}$$

where the error definition for CMA, which is different from the error definitions of other algorithms, is as follows

$$\varepsilon(n) = (|y(n)|^2 - y_0^2)y(n) \tag{3.31}$$

According to [16], the algorithm has the fastest speed of convergence for the following choice of the step size

$$\mu = \frac{1}{\left[\frac{1}{L}\sum_{i=k}^{k+L-1} 6\lambda_{\max}^2(i)\right]} \tag{3.32}$$

and λ_{max} is the maximum eigenvalue of the correlation matrix **R**

$$\mathbf{R}(n) = \underline{x}(n)\underline{x}^H(n) \tag{3.33}$$

Development of CMA for beam-space array signal processing, including its hardware realization, has been reported in [12]. The results presented in [12] indicate that the beam-space CMA is able to cancel interferences arriving from directions other than the look direction. However, since there is no a priori knowledge of the desired signal, the algorithm may direct the array beam to a constant envelope but not to the desired signal in the environment. Initial choice of weight vector may direct the array pattern toward the undesired signal, which is constant envelope as well. In that case, the array converges to that undesired signal. Therefore, the choice of the initial weight vector affects the convergence of the algorithm considerably.

CHAPTER 4

MODELLING OF MUTUAL COUPLING EFFECTS IN ANTENNA ARRAYS

The radiation pattern of an array antenna is computed to be the product of the array factor and the element pattern provided that each array element is identical and assumed to be isolated. Unfortunately that may be true for only antenna arrays with large separation distances (d~λ).

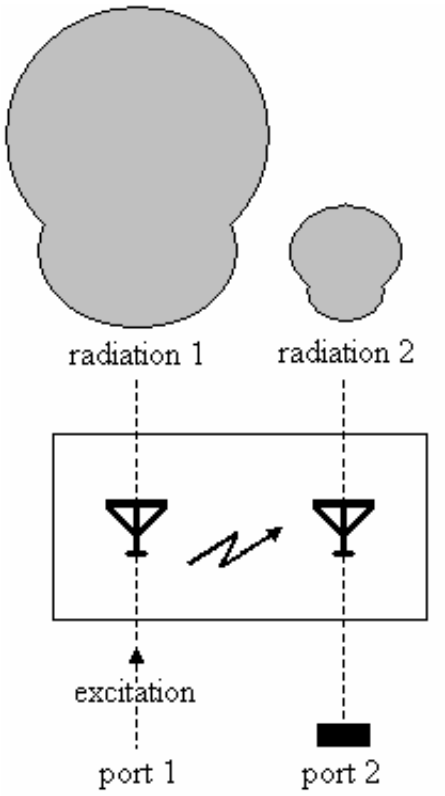

Figure 4.1 Two port antenna network

Radiation pattern of an individual element in closely spaced arrays is affected from other array elements that act as scatterers. As an example, consider the two element array antenna that have small interelement spacing shown in Figure 4.1. This system can be considered as a two port distributed element network. When the first antenna element is excited and the second antenna is terminated with matched load, the first antenna element generates the radiation pattern 1. Since some of the energy is coupled through the radiation pattern of the first element to the second, a current will be induced on the second element. Therefore the second element also radiates, even though it is not excited. This effect is shown by radiation 2 in the same figure. The two elements are assumed to be identical thus have similar radiation patterns. The more the energy coupled to the other element the stronger the radiation pattern it generates. Therefore, due to mutual coupling, the active radiation pattern, which is the radiation pattern of an array element when the other elements are terminated with matched loads, is not merely the first radiation pattern but a combination of both patterns. Therefore the mutual coupling between the array elements should be considered in order to correctly simulate the measured signals at the input of the antenna elements.

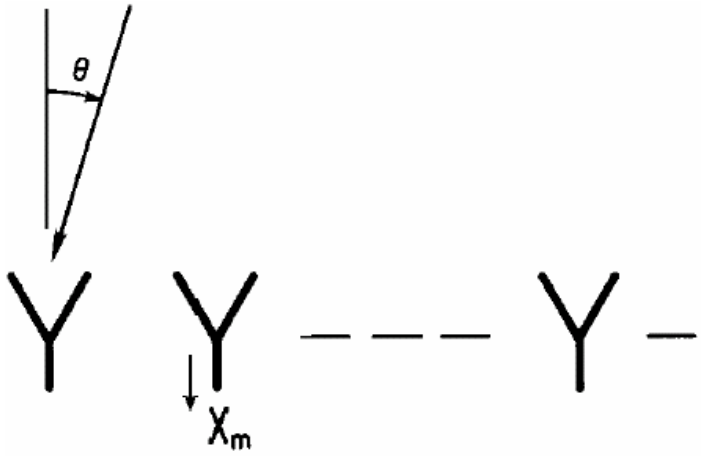

Figure 4.2 Mutual Coupling in a linear array

Considering the n-element linear array shown in Figure 4.2, the measured signal vector without mutal coupling can be written as follows:

$$[X]^{no\_MC} = \begin{bmatrix} 1 \\ e^{jkdu} \\ \vdots \\ e^{jkndu} \end{bmatrix} \tag{4.1}$$

where d is the interelement spacing for the equispaced array, u is the sine of the angle θ from broadside. In order to simulate the measured signals with mutual coupling, the scattering matrix of the array will be used.

The entire coupling behaviour of an N port array, as shown in Figure 4.3, can be characterized by an NxN scattering matrix, [S].

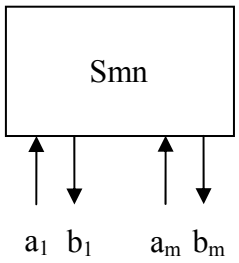

Figure 4.3 Scattering parameters of N port network

where 'a' denotes the waves incident to the ports and 'b' denotes the waves reflected from the ports where they are related to each other by the scattering matrix [S]:

$$[b] = [S] \cdot [a] \tag{4.2}$$

The measured signals with mutual coupling at the input of the n^{th} element is the superposition of the incident and reflected waves:

$$X_n^{MC} = a_n + b_n$$

$$= a_n + \sum_{m=1}^{N} s_{nm} a_m$$

$$= \sum_{m=1}^{N} (\delta_{nm} + s_{nm}) a_m$$

$$[X]^{MC} = \{[I] + [S]\}[a] = [C][a] \tag{4.3}$$

where [C] is defined as the array coupling matrix. Using the fact that [a]=[x]no_MC, the measured signals under mutual coupling can be related to the measured signalswithout mutual coupling as follows:

$$[X]^{MC} = [C][X]^{no\_MC} \tag{4.4}$$

In most of the antenna arrays used in practice, the scattering matrix can either be measured or computed by using an electromagnetic simulation tool like Numerical Electromagnetics Code (NEC) for dipole arrays or ENSEMBLE by Ansoft for microstrip antenna arrays. Therefore the coupling matrix can be easily obtainted to simulate the measured signals under mutual coupling conditions.

It should be noted that the method obtained above is applicable only to antenna arrays with single mode elements. Single mode elements are scan-independent i.e. the current distribution on their aperture changes only in magnitude but not in shape for different directions. A single coupling matrix may be computed, which is valid for all directions, to update excitation coefficients.

The adaptive array algorithms work with the measured signals. When the strong mutual coupling between the antenna elements degrades the performance of an adaptive array, the mutual coupling effects can be easily eliminated. The measured signal vector should be multiplied with the inverse of the coupling matrix to obtain the signal vector without mutual coupling. Then this signal vector can be used as an input for the adaptive algorithms.

CHAPTER 5

SIMULATION RESULTS AND DISCUSSIONS

Computer simulations are performed to study the performance of adaptive algorithms that are explained in Chapter 3. First the adaptive algorithms are studied by considering no mutual coupling between array elements and their performances are compared. Next, the effects of mutual coupling is included in the simulations by using the scattering matrices of microstrip antenna arrays which are obtained from the electromagnetic simulation tool called Ensemble by Ansoft.

During the simulations, the communication problem shown in Figure 5.1 is used. Two signal sources situated at the far field of a two element antenna array is shown in Figure 5.1. The simulations are also performed for three element arrays with two interfering sources.

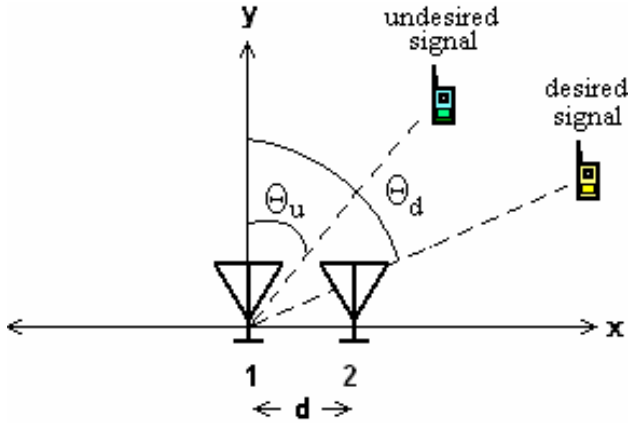

Figure 5.1 Two element adaptive array structure

Θ_d and Θ_u denote the angles that the broad side of the array makes with the desired and the undesired signals, respectively. The desired signal corresponds to the mobile user that the base station wants to communicate. The undesired signal represents another mobile user communicating within the same frequency band of the desired user. Therefore the undesired signal causes a co-channel interference for the desired signal.

The received signals on each antenna element will have three components which can be expressed as follows

$$x_i = d + u + n_i \qquad i=1,2 \qquad (5.1)$$

where d represents the desired signal, u is the undesired signal and n_i is the additive white gaussian noise (AWGN) received at the i^{th} element. In the simulations of the non-blind algorithms, the desired signal is taken as the reference signal.

The block diagram of the MATLAB program developed for the simulations is shown in Figure 5.2.

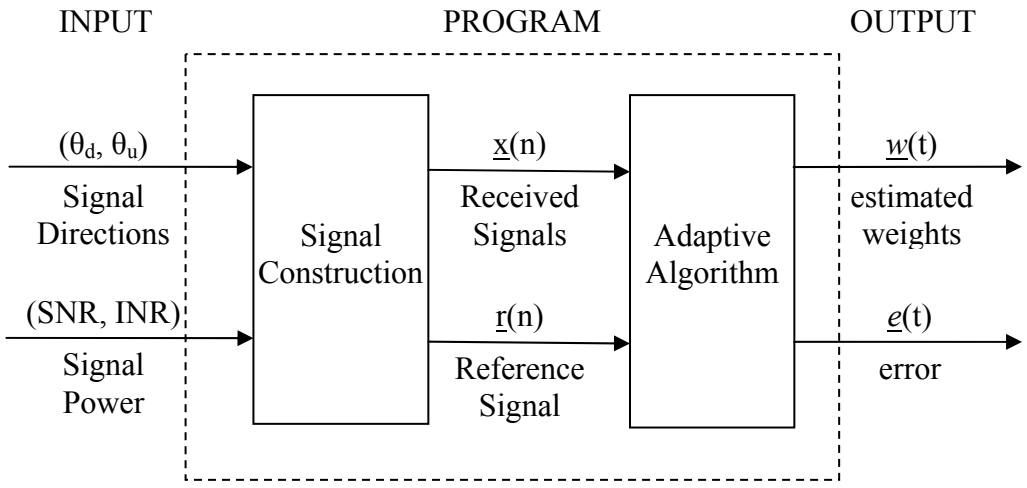

Figure 5.2 The Block Diagram of the MATLAB programs

The signal to noise ratio (SNR) and interference to noise ratio (INR) values are the desired signal to noise and undesired signal to noise ratios, respectively.

According to the given input values (Θ_d, Θ_u, SNR, INR) the signal construction subroutine generates the received signal sequences (time samples). During the construction of the signals, first the information data of each user is produced. Since both signals occupy the same frequency band, the desired and undesired signals are multiplied by different PRN (pseudo random noise) codes randomly in order to achieve multiple access. PRN codes are also generated randomly and the code length is chosen to be 32 bits with 4 bits per symbol. Next, the coded desired and undesired signals are modulated by quadrature phase shift keying (QPSK) type modulation.

The modulation type of the system is chosen to be 4-QPSK. In QPSK, the phase of the carrier takes on one of four equally spaced values, 0, π/2, π, 3π/2, according to the coded information signal.

The modulated signals pass through the pulse shaping filter which characterizes the bandwidth of the transmission channel. That is modelled as shown in Figure 5.3.

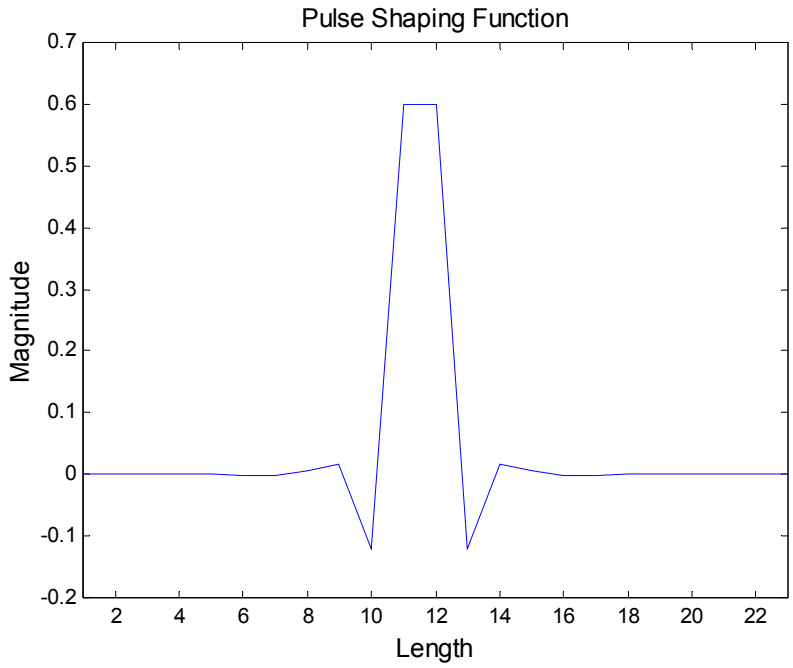

Figure 5.3 The pulse shaping function

Finally, the zero mean white gaussian noise is added to these signals and the received signal sequences, $x_i(n)$, are obtained. Note that the desired signal and the undesired signal induced on the i^{th} element will have a phase shift of $e^{j(i-1)d\sin\Theta d}$ and $e^{j(i-1)d\sin\Theta u}$, respectively.

The received signals and the reference signal generated by the signal construction subroutine are the inputs of the adaptive algorithm subroutine. The outputs of the adaptive algorithms are the estimated weights and the error between the output of the array and the reference signal. Recall that the non-blind algorithms utilize the reference signal whereas the blind algorithm CMA makes use of the constant amplitude property of the modulated signal.

In QPSK type modulation, the amplitude of the modulated signal is kept constant [19]. Therefore, this type of modulation is suitable for the implementation of CMA algorithm. To demonstrate this fact, the total received signal and only the desired signal part of the received signal are plotted in Figures 5.4 and 5.5, respectively.

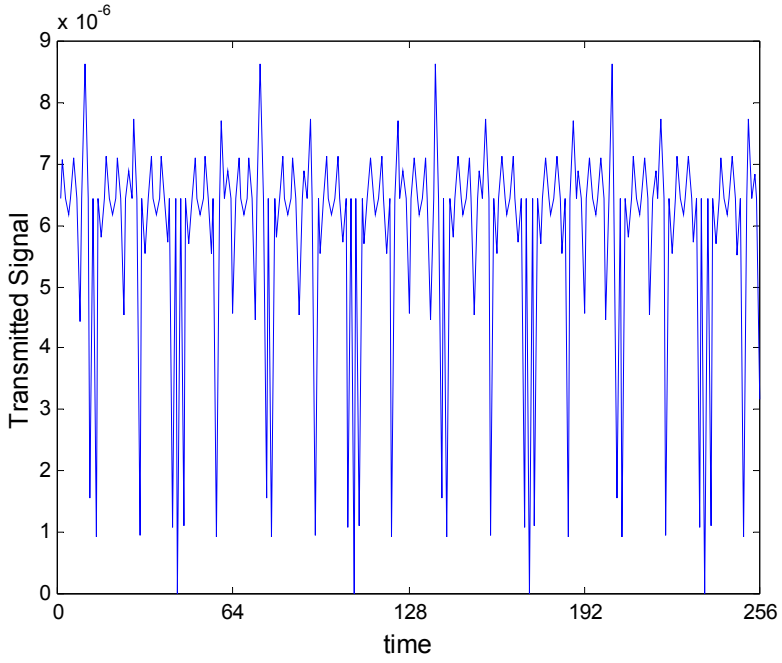

Figure 5.4 The amplitude of the desired signal (Θ_d=30 ^{o}, Θ_u=-30^o SNR=10dB, INR=0dB)

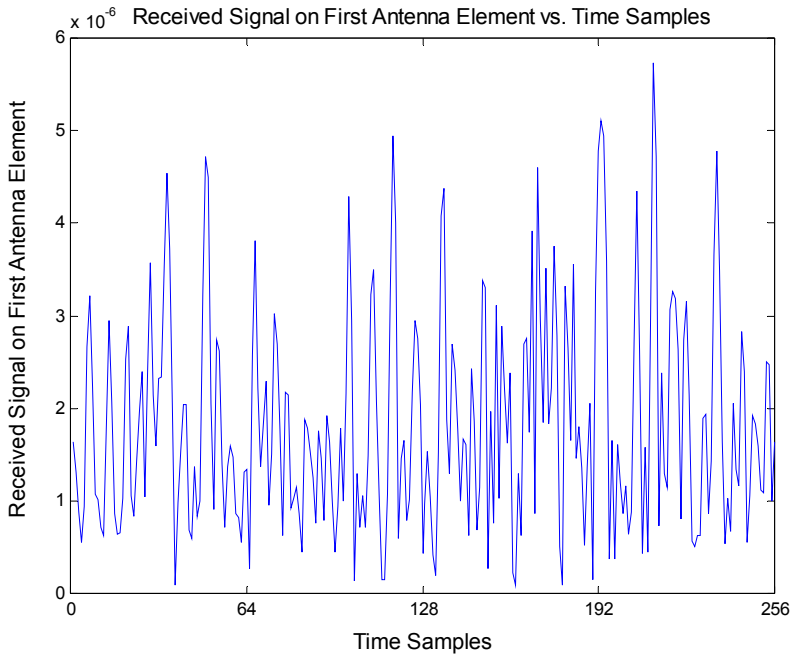

Figure 5.5 The amplitude of the received signal on first antenna element (Θ_d=30^o, Θ_u= −30^o SNR=10dB, INR=0dB)

It is observed from Figure 5.4 that the constant amplitude property of the desired signal is distorted slightly due to the characteristics of the pulse shaping filter. This may result in some convergence problems for CMA algorithm. To avoid this problem, instead of a single time sample of the received signal, an average of L time samples are used as described in section 3.2.1.

As it can be seen from Figure 5.5, the amplitude of the recived signal which is a superposition of desired and interfering signals varies significantly. Therefore by invoking the constant amplitude condition on the received signal, the interfering signal can be suppressed.

In the following section, automatic interference suppression characteristics of both blind and non-blind algorithms will be demonstrated by presenting the array patterns calculated by using the estimated weights obtained from different algorithms.

5.1 INTERFERENCE SUPPRESSION

In the adaptive algorithm subroutine section, weights for the antenna elements are estimated using adaptive algorithms LMS, CGM, RLS and CMA. The radiation patterns computed by using the estimated weights obtained at the last iteration of each algorithm are presented in Figure 5.6.

As stated previously, the non-blind adaptive algorithms try to minimize the MSE between the array output and the reference signal. It can be seen from Figure 5.6 that all of the algorithms form their radiation patterns in order to direct the main beam toward the desired signal and place a null toward the interfering signal source.

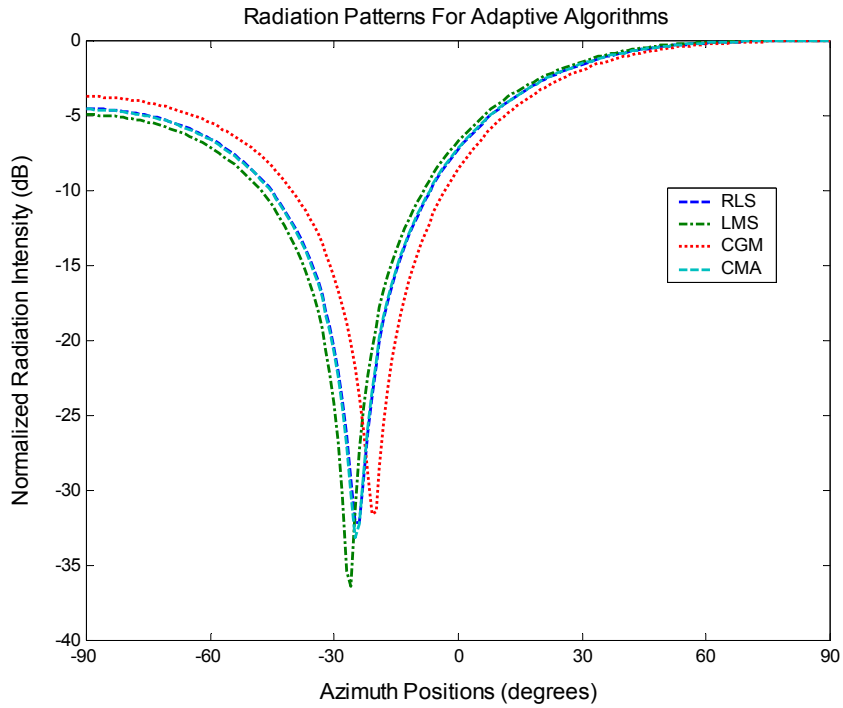

Figure 5.6 Radiation patterns for adaptive algorithms using estimated weights (Θ_d=20^o, Θ_u= −20^o, SNR=20dB, INR=20dB)

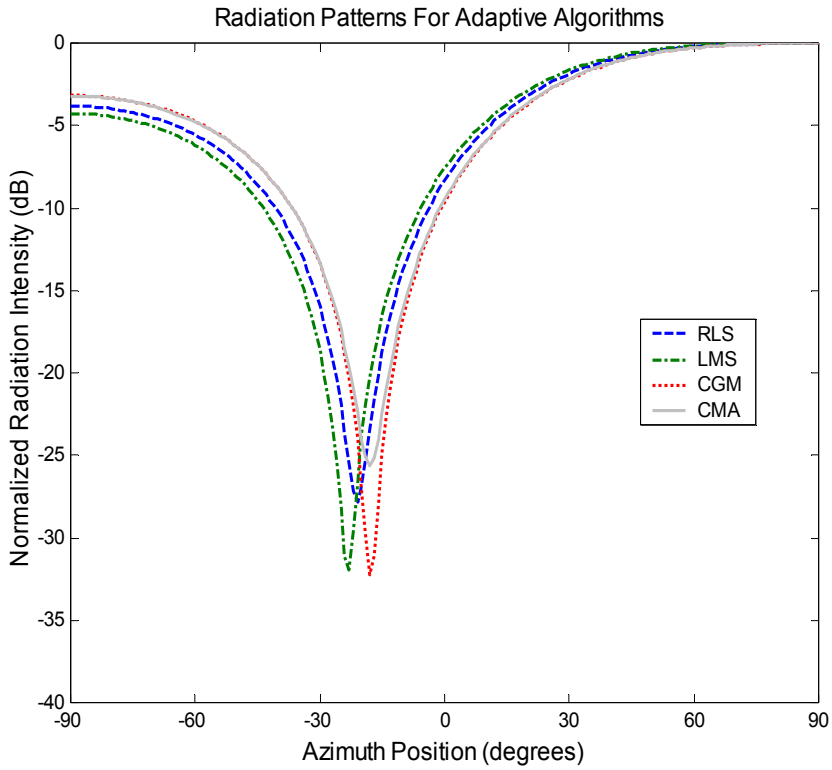

Figure 5.7 Radiation patterns for adaptive algorithms using estimated weights (Θ_d=20°, Θ_u= −20°, SNR=20dB, INR=30dB)

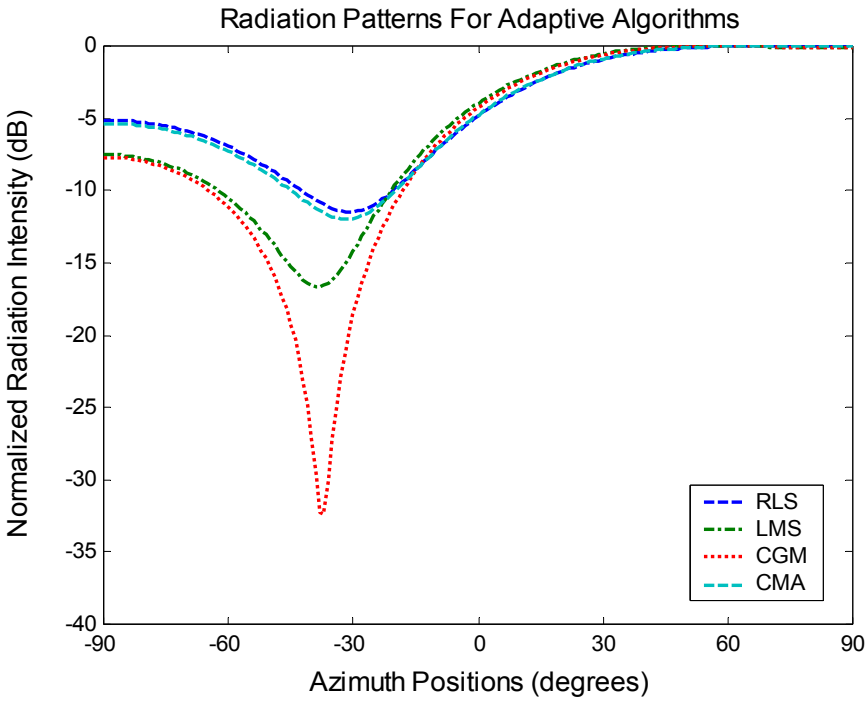

Figure 5.8 Radiation patterns for adaptive algorithms using estimated weights

Θ_d=20°, Θ_u= −20°, SNR=20dB, INR=10dB)

The result of minimizing the MSE is observed as trying to increase the signal reception from the desired signal and decrease the signal reception from the interfering sources. In Figures 5.6, 5.7 and 5.8 the radiation patterns for different SNR, INR couples are illustrated. Note that, all of the algorithms place a deeper null (~35dB) in the direction of the interferer when the interference power is higher than the desired signal power. However when the case is reversed, the depth of the null in the direction of the interference signal decreases. LMS places 15dB, both CMA and RLS place 12dB nulls while the depth of the null with CGM changes only very slightly. Moreover, the angle of null positions get worse with smaller interferer power. It can be concluded that with increasing interferer power, the algorithms prefer to form patterns which try to decrease the signal reception from the interferer.

For a two element antenna array as in our problem, the system has one degree of freedom. The system prefers either to put a deeper null toward the interferer or to increase the amount of power from the desired source. For antenna arrays with more array elements, the required number of elements in the array should be more than the number of array operations at least by one. Consider a communication system with 2 desired signal sources and 3 co-channel interferers. In order to maximize the signal reception from all of the desired sources and minimize all of the interfering signals, the antenna array should have at least 6 elements.

5.2 PERFORMANCE COMPARISONS OF ADAPTIVE ALGORITHMS

The speed of convergence and the improvement in the received signal to interference plus noise ratio (SINR) yield information about the capability of the MSE minimization of the adaptive algorithms. In this thesis, when making performance comparisons, these two criteria have been used to investigate the performance of the adaptive algorithms.

All of the algorithms are tested for the same set of received signals and the

simulations are carried out over 100 different sets of generated signals. Therefore in addition to averaging over the time samples also the average of 100 different simulations are considered. During the simulations, the gradient step size for LMS is chosen $0.9/T_r(\mathbf{R})$ as in agreement with the expression stated in 3.1.1. The forgetting factor in the RLS algorithm is taken simply to be 0.5 and epsilon is chosen as 0.01.

5.2.1 Weight Convergence of the Adaptive Algorithms

The convergence of the real and imaginary parts of the weights for both of the array elements are shown in figures 5.9, 5.10, 5.11 and 5.12 for each algorithm under inspection.

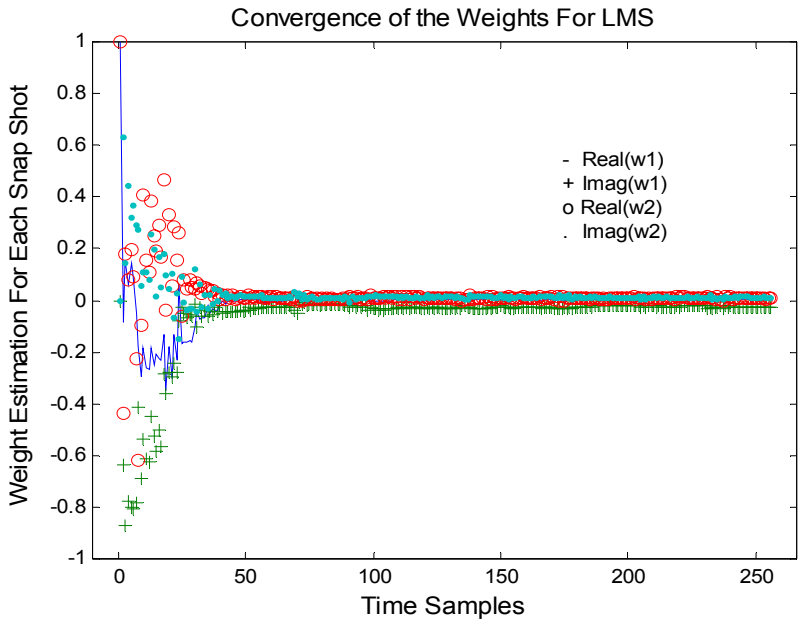

Figure 5.9 Convergence of weights in LMS ($\Theta_d = 20^o$, $\Theta_u = -20^o$, SNR=20dB, INR=20dB)

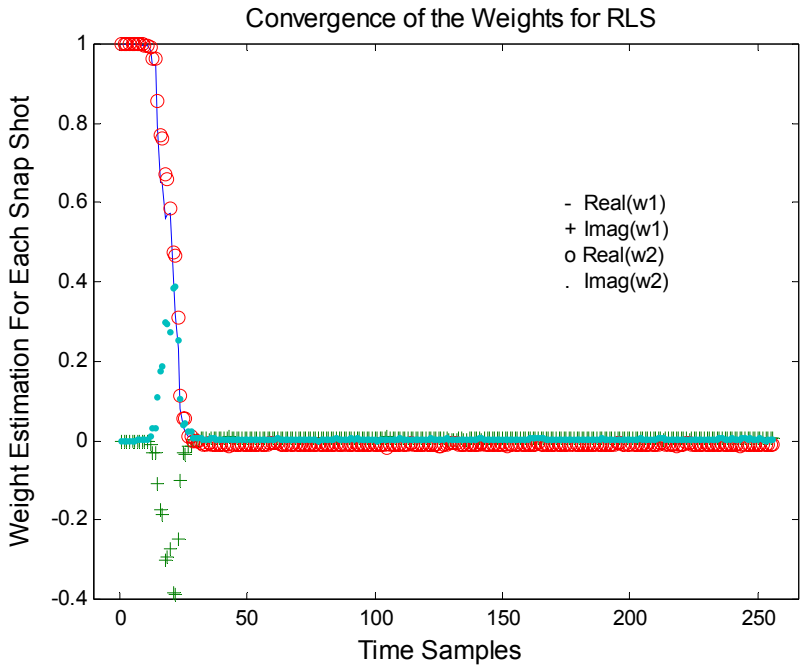

Figure 5.10 Convergence of weights in RLS ($\Theta_d = 20^o$, $\Theta_u = -20^o$, SNR=20dB, INR=20dB)

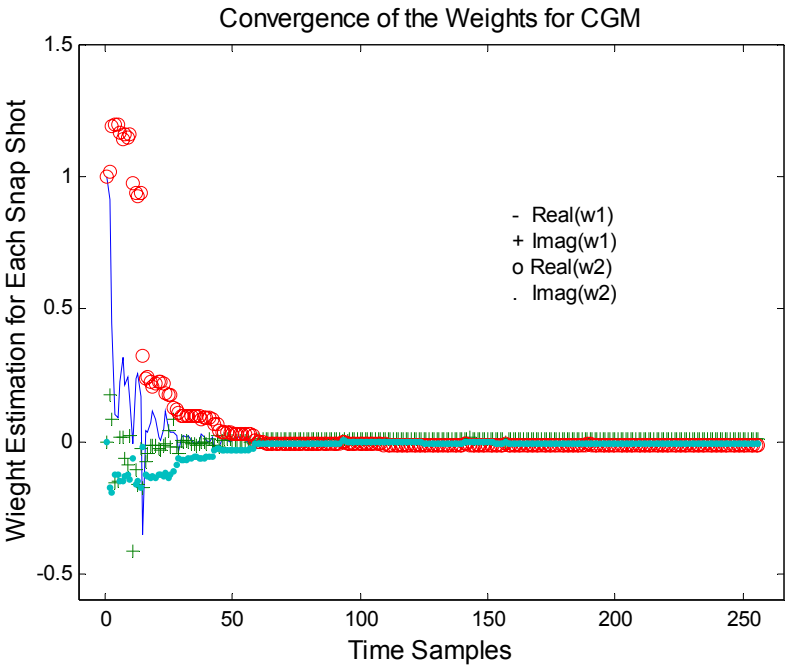

Figure 5.11 Convergence of weights in CGM ($\Theta_d = 20^o$, $\Theta_u = -20^o$, SNR=20dB, INR=20dB)

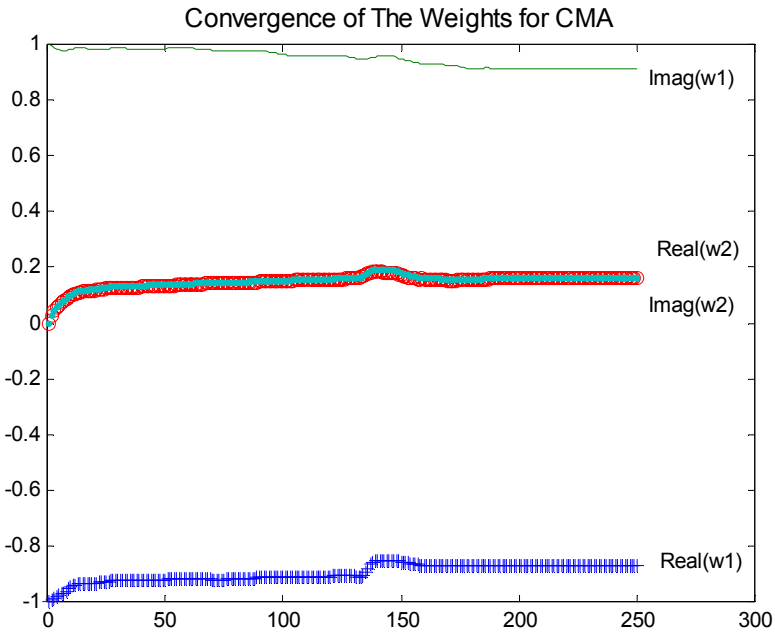

Figure 5.12 Convergence of weights in CMA ($\Theta_d = 20^o$, $\Theta_u = -20^o$, SNR=20dB, INR=20dB)

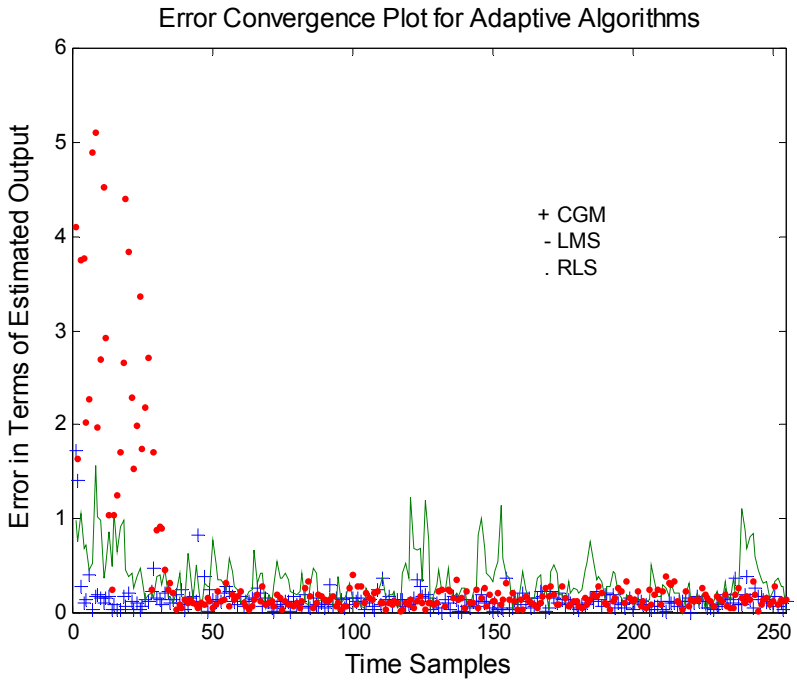

Figure 5.13 Error in Non-Blind Algorithms ($\Theta_d = 20^o$, $\Theta_u = -20^o$, SNR=20dB, INR=20dB)

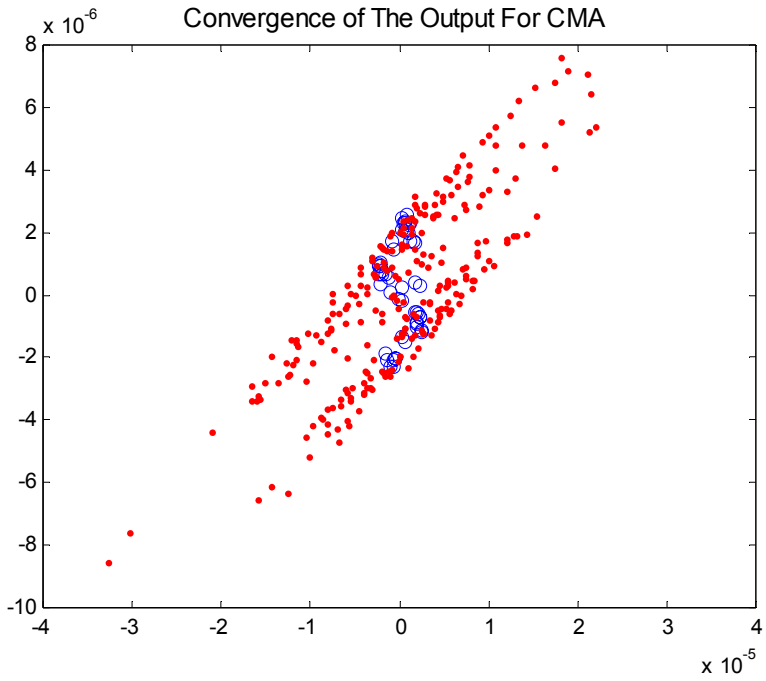

Figure 5.14 Convergence of the output for CMA ($\Theta_d = 20^o$, $\Theta_u = -20^o$, SNR=20dB, INR=20dB)

The error definitions for LMS, RLS and CGM are the same and different than that of CMA. Figure 5.13 depicts the error between the estimated output and the reference signal for adaptive algorithms except CMA. Figure 5.14 depicts the distribution of measured signals and estimated outputs on the same plot. Note that the output values are closely spaced when compared with the input data which intuitively express the convergence of the CMA. There is no definite convergence to a certain value. Hence it is obvious that CMA cannot perform as well as non-blind algorithms since no reference signal is utilized. In RLS , the weights converge to the optimal solution but it is a bit late than the other algorithms. In other words, it is expected that the error done at early time steps for RLS is large. From the figures, it is also explicit to note that the CGM convergence is the most stable of all the other algorithms.

The ensemble-averaged squared error values for each algorithm are presented in sections 5.2.1.1 and 5.2.1.2 for different number of array elements and interfering source combinations with different SNR and INR couples.

5.2.2 Speed of Convergence of the Adaptive Algorithms

Figure 5.6 - 5.8 display the radition patterns generated by using the estimated weights at the last iteration of the algorithms. Figure 5.9 - 5.14 demonstrate how the estimated weights converge to the optimal Wiener-Hopf solution. It is seen that all of the algorithms present expected results. But it is impossible to make a judgement for the accuracy of the ultimate convergence. To make a quantitative comparison, the error done at each algorithm should be used.

Table 5.1 ($\Theta_d=20^o$, SNR=20dB), 1 interferer INR= 30dB, 2 array element

	MC State	Iteration Set	LMS	RLS	CGM	CMA
$\Theta_u= 10^o$	With MC	1..25	10.5979	127.6139	3.7211	14.0466
		26..50	4.0193	2.3650	1.8822	10.6048
		51..75	4.4548	0.7372	1.7402	13.5995
		100..255	2.0038	0.6655	0.8907	10.4862
		206..255	1.7471	0.6403	0.7021	10.5668
	Without MC	1..25	4.7406	106.9917	2.6287	3.7815
		26..50	2.0266	3.1360	0.9842	3.5372
		51..75	1.7568	0.7253	0.8766	3.2733
		100..255	1.4704	0.6606	0.6739	2.6232
		206..255	1.4546	0.6333	0.6376	2.6002
$\Theta_u= -70^o$	With MC	1..25	0.4611	3.6223	0.1468	3.1756
		26..50	0.0456	0.4137	0.0126	3.0944
		51..75	0.0454	0.0229	0.0111	3.3136
		100..255	0.0469	0.0232	0.0127	2.6132
		206..255	0.0480	0.0233	0.0131	1.4958
	Without MC	1..25	0.3391	2,5152	0.1195	1.4074
		26..50	0.0323	0.3753	0.0141	0.8844
		51..75	0.0381	0.0239	0.0122	0.7344
		100..255	0.0368	0.0229	0.0136	0.3985
		206..255	0.0372	0.0225	0.0125	0.3126

Tables 5.1, 5.2 and 5.3 tabulate the ensemble-averaged squared error values for four of the adaptive algorithms with various communication scenarios. The iteration set column presents results for different set of ensemble-averaged squared error values within the iteration interval specified. All of the error values are averaged over 100 runs. For the problems inspected in all of the three tables, the desired signal is kept constant at 20^o with 20dB desired signal to noise ratio. For all of the communication scenarios, the results are obtained for the measured signal with mutual coupling and data without mutual coupling.

The scattering matrix of the two element microstrip antenna array is computed by ENSEMBLE and the following matrix is obtained,

$$s = \begin{bmatrix} 0.0971\angle 14.064 & 0.42606\angle -19.305 \\ 0.42606\angle -19.305 & 0.09793\angle -41.248 \end{bmatrix} \tag{5.2}$$

Table 5.1 compares results for different interferer positions where the first set is obtained when the undesired signal is at 10^o with the case when the undesired signal is at -70^o.

As it is expected, all of the algorithms perform better as the angular separation between the desired and interfering signals gets larger. The accuracy of both CGM and RLS improves about 60-65% when the interferer is far away from the desired source. It is also observed that the reduction in the accuracy of LMS is far more than the reduction in the accuracy of these two algorithms. The effect of mutual coupling is negligible for all of the there non-blind methods.

Among the non-blind algorithms, LMS is the most inaccurate and CGM is the most accurate when the average of last 50 iterations are considered. The method of steepest descent often travels through the same directions as earlier iterations as shown in Figure 3.2 and as stated in section 3.1.3, the direction vector of the previous iteration and the error vector of the previous iteration in CGM are **A** orthogonal depending on the fact that new search direction should be in the same direction as the error vector. Therefore it is not suprising that the accuracy of the

CGM is higher than both LMS and RLS. RLS is also a steepest descent based algorithm. Hence its accuracy is lower than CGM. When the ensemble averaged-squared errors are compared for the first 50 iterations, it is observed that LMS and CGM converges faster than the RLS. This result can be attributed to the fact that RLS is a method that utilizes the measured signals of the previous time samples as well as the current one. Therefore the error done in the previous iterations may propagate. On the other hand, since this property provides a better estimation of **R** matrix when the number of iterations are increased, the accuracy of RLS becomes more accurate. Thus RLS is more accurate than LMS.

Although the error in CMA is larger than the error in non-blind algorithms, it can be observed that the ensemble averaged-squared error decreases with each iteration which implies the convergence of the algorithm.

The non-blind algorithms make use of a reference signal. Therefore, whether the measured signal is affected by mutual coupling or not, these algorithms always converge to a set of weights that matches the array output to the reference signal. The converged weights might be different when there is mutual coupling; however, the proper weight set can be computed. Hence mutual coupling does not affect the performance of these algoritms considerably. On the other hand, since CMA does not utilize a reference signal, it is harder for it to converge to the optimal solution that matches the array output to the intended signal. Consequently, accuracy and speed of convergence of CMA are severly degraded under mutual coupling.

Table 5.2 compares results for different interferer powers where the first set is obtained when the undesired signal has 30dB, and the second has 10dB interferer to noise ratios. At each case, the interferer is located at 10^{o}. The desired signal is kept constant at 20^{o} with 20dB desired signal to noise ratio as before.

Table 5.2. (Θ_d=20^o, SNR=20dB), 1 interferer Θ_u= 10^o, 2 array element

	MC State	Iteration Set	LMS	RLS	CGM	CMA
INR=30dB	With MC	1..25	10.5979	127.6139	3.7211	14.0466
		26..50	4.0193	2.3650	1.8822	10.6048
		51..75	4.4548	0.7372	1.7402	13.5995
		100..255	2.0038	0.6655	0.8907	10.4862
		206..255	1.7471	0.6403	0.7021	10.5668
	Without MC	1..25	4.7406	106.9917	2,6287	3.7815
		26..50	2.0266	3.1360	0.9842	3.5372
		51..75	1.7568	0.7253	0.8766	3.2733
		100..255	1.4704	0.6606	0.6739	2.6232
		206..255	1.4546	0.6333	0.6376	2.6002
INR=10dB	With MC	1..25	0.5902	4.9557	0.4100	1.7555
		26..50	0.5640	0.5919	0.3635	1.5079
		51..75	0.5086	0.2577	0.3015	1.6499
		100..255	0.4857	0.2489	0.2715	1.6908
		206..255	0.4943	0.2463	0.2813	1.7171
	Without MC	1..25	0.5397	4.2358	0.2168	1.3063
		26..50	0.4638	0.5816	0.1787	1.3206
		51..75	0.3935	0.2368	0.1554	1.2702
		100..255	0.4296	0.2466	0.1632	1.2992
		206..255	0.4248	0.2447	0.1617	1.2893

The discussions made about the speed of convergence, accuracy and mutual coupling effects of the algorithms with regard to table 5.1 are similar for Table 5.2. The CGM is the most accurate where the LMS is the least. As far as the speed of convergence is concerned, the RLS is the slowest and the CGM is the fastest of the algorithms. Mutual coupling effect is negligible in RLS and not more than 15% in CGM and LMS. CMA is also convergent but the accuracy is poor as in the previous case.

It is clear that, when the interferer power gets lower, the accuracy of the algorithms are better which is an expected case. Suppressing a more powerful interferer is harder.

Table 5.3. (Θ_d=20^o, SNR=20dB), 1 interferer Θ_u= 10^o, INR=30dB

	MC State	Iteration Set	LMS	RLS	CGM	CMA
2 array elements	With MC	1..25	10.5979	127.6139	3.7211	14.0466
		26..50	4.0193	2.3650	1.8822	10.6048
		51..75	4.4548	0.7372	1.7402	13.5995
		100..255	2.0038	0.6655	0.8907	10.4862
		206..255	1.7471	0.6403	0.7021	10.5668
	Without MC	1..25	4.7406	106,9917	2,6287	3.7815
		26..50	2.0266	3,1360	0.9842	3.5372
		51..75	1.7568	0.7253	0.8766	3.2733
		100..255	1.4704	0.6606	0.6739	2.6232
		206..255	1.4546	0.6333	0.6376	2.6002
3 array elements	With MC	1..25	7.3949	521.2846	2.3752	7.5763
		26..50	0.8611	2.7927	0.3998	4.0416
		51..75	0.5849	0.2601	0.2107	3.3917
		100..255	0.5033	0.2564	0.1294	2.8426
		206..255	0.4992	0.2576	0.121	2.8377
	Without MC	1..25	4.676	163.2087	1.7091	6.0160
		26..50	0.5685	2.013	0.278	2.7973
		51..75	0.4624	0.2265	0.1461	2.2745
		100..255	0.3872	0.2146	0.1134	1.7215
		206..255	0.388	0.2146	0.1114	1.7711

In table 5.3 the undesired signal has 30dB interferer to noise ratio while it is located at 10^o. The desired signal is kept constant at 20^o with 20dB desired signal to noise ratio as before. But this time the array elements is increased by one which also indicates an increase in degree of freedom of the system by one.

The scattering matrix obtained for the three element array is as follows:

$$s = \begin{bmatrix} 0.05844\angle 12.49 & 0.397\angle 64.9 & 0.141\angle -39.63 \\ 0.397\angle -64.9 & 0.14\angle 19.73 & 0.389\angle 70.2 \\ 0.141\angle -39.63 & 0.389\angle 70.2 & 0.126\angle 38.29 \end{bmatrix} \quad (5.3)$$

In this scenario, the results are improved drammatically. Accuracy is improved by nearly 65% in CGM, by 40% in RLS and by more than 100% in

LMS.

The convergence speed and accuracy comparison between the algorithms are not changed. The CGM is the most accurate where the LMS is the least. The RLS is the slowest and the CGM is the fastest of the algorithms. Mutual coupling effect is still low in non-blind algorithms. CMA is also convergent but the accuracy is poor, also the mutual coupling effects the performance parameters much as in the previous cases.

Table 5.4. (Θ_d=20^o, SNR=20dB), 2 interferers Θ_{u1}= 10^o, INR1=30dB, Θ_{u2}= 30^o, INR2=20dB

	MC State	Iteration Set	LMS	RLS	CGM	CMA
2 array elements	With MC	1..25	9.6787	96.4105	5.3949	17.2116
		26..50	6.973	2.6652	3.5833	12.6232
		51..75	8.661	1.7691	4.418	12.4422
		100..255	6.2384	1.737	4.0594	10.1345
		206..255	6.0593	1.7122	3.9967	11.7629
	Without MC	1..25	5.642	91.5731	4.3966	4.6872
		26..50	3.8461	3.3821	3.0898	3.9212
		51..75	5.3604	1.8216	3.2093	3.1342
		100..255	4.8559	1.724	3.4648	2.1152
		206..255	4.5571	1.7064	3.2259	2.2231
3 array elements	With MC	1..25	5.7672	79.2529	5.6583	9.8508
		26..50	3.4142	3.3302	2.8188	3.1191
		51..75	3.3329	1.4492	2.9277	1.7794
		100..255	2.7319	1.4436	2.5745	1.6645
		206..255	2.526	1.4186	2.4649	1.5350
	Without MC	1..25	5.1315	66.8527	3.4217	7.0641
		26..50	3.0331	2.7818	1.9026	2.7611
		51..75	2.8499	1.0794	1.7983	1.5605
		100..255	2.2755	1.0606	1.4769	1.7391
		206..255	2.0439	1.0667	1.3656	1.6507

Table 5.4 investigates the accuracy of MSE minimization when a second interfering source is present in the environment while the desired signal is situated

at 20^o with 20dB SNR. The results of antenna array with two elements and antenna array with three elements are compared.

By comparing Table 5.1 which display results for $\Theta_{u1}= 10^o$, INR=30dB with Table 5.4 where a second interferer is located in the vicinity of the desired signal with $\Theta_{u2}= 30^o$, INR2=20dB, it is observed that all of the ensemble averaged-squared errors severly grew in the latter case while the speed and the final accuracy characteristics of the algorithms remained relatively costant. Increasing antenna element by one reduces the errors significantly.

LMS is the least accurate and RLS is the slowest as in the previous scenarios. But interestingly, RLS is more accurate than CGM. The expectation operator for the RLS provides better estimation when the degree of interference is increased at the measured signals. As stated previously, RLS utilizes past estimates together with the instantaneous noisy estimates rather than utilizing only instantaneous noisy estimates. Besides, CMA results are improved very little when the number of antenna elements in the array is increased by one.

It is easier to observe the speed and accuracy of the RLS algorithm with increasing time samples considering the interferer location. Figure 5.15 displays ensemble averaged-squared error value distribution for different interferer locations from -70^o to 70^o for each set of iterations. The desired signal is located at 20^o with 20dB SNR. For first 25 time samples the error is larger than the other set of samples inspected. And when the number of iterations is increased, the algorithm results with smaller error when the interferer is closer to the desired signal.

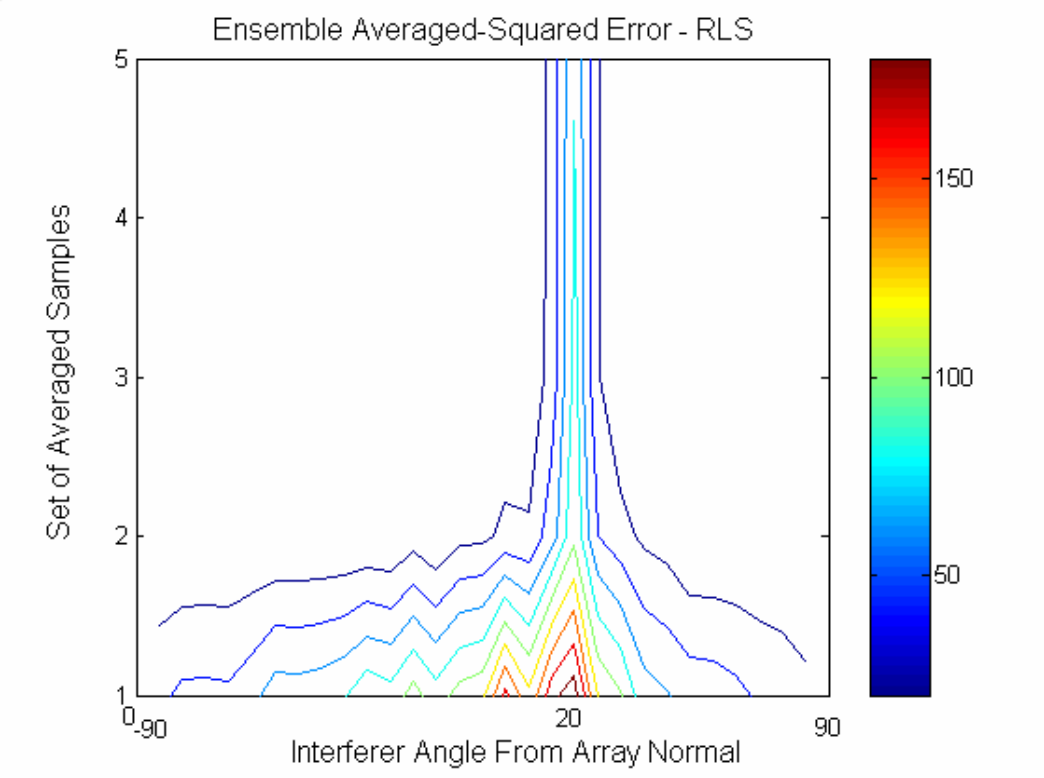

Figure 5.15 Ensemble Averaged-Squared Error for different spatial locations considering different set of time samples

5.2.3 SINR Performance in the Adaptive Algorithms

Another measure to determine whether an adaptive algorithm has ended up with a proper weight vector which minimizes MSE is to investigate the SINR performance at the output of the system. The output SINR, for problem given in Figure 5.2 is:

$$SINR = \frac{\text{Received Desired Power}}{\text{Received Undesired Power + Received Noise}}$$

$$= \frac{\underline{w}^H \underline{d}\,\underline{d}^H \underline{w}}{\underline{w}^H \underline{u}\underline{u}^H \underline{w} + \underline{w}^H \underline{n}\underline{n}^H \underline{w}} \tag{5.4}$$

Figure 5.16 displays output SINR values obtained using the last weight vector estimated by each algorithm on the same plot. Figure 5.17 displays the same plot with Figure 5.16 except the input signal data is effected by mutual coupling.

During the calculation of the SINR at the output of the array, the direction of the desired signal is kept constant at 0^o with SNR 20dB and the direction of the interferer is swept from -90^o to 90^o. It is observed that the SINR values gets smaller as the interferer gets closer to the desired signal location, i.e. in order to have the same quality of communication when the interfering signal is close to the desired signal, the transmitted signal strength should be increased. When the SINR values are compared, it is observed that CGM outperforms all of the algorithms and RLS is better than both LMS and CMA. This conclusion is expected on the premise of the results obtained from the convergence of ensemble averaged-squared error values.

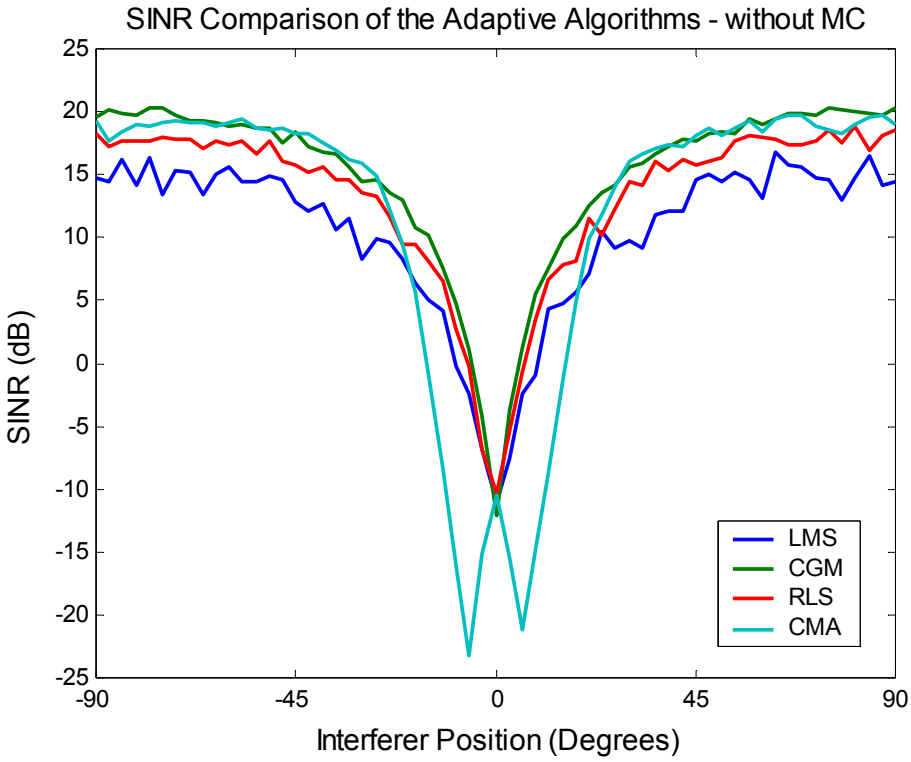

Figure 5.16 SINR pattern with respect to Θ_u without MC ($\Theta_d = 0^o$, SNR=20dB, INR=20dB)

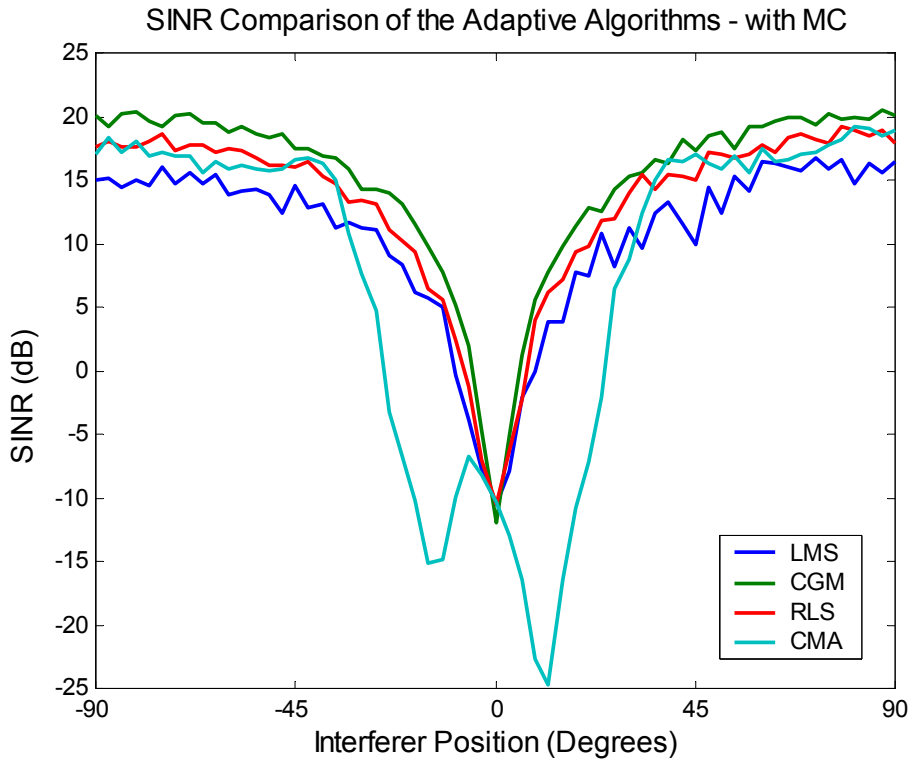

Figure 5.17 SINR pattern with respect to Θ_u ($\Theta_d = 0^o$, SNR=20dB, INR=20dB)

To understand the effect of mutual coupling clearly, consider the Figures 5.18-5.21 where the SINR patterns for data with and without mutual coupling are displayed separately for each algorithm. It is observed that the mutual coupling does not deteriorate the performance of SINR in non-blind algorithms. But it affects the performance for CMA much.

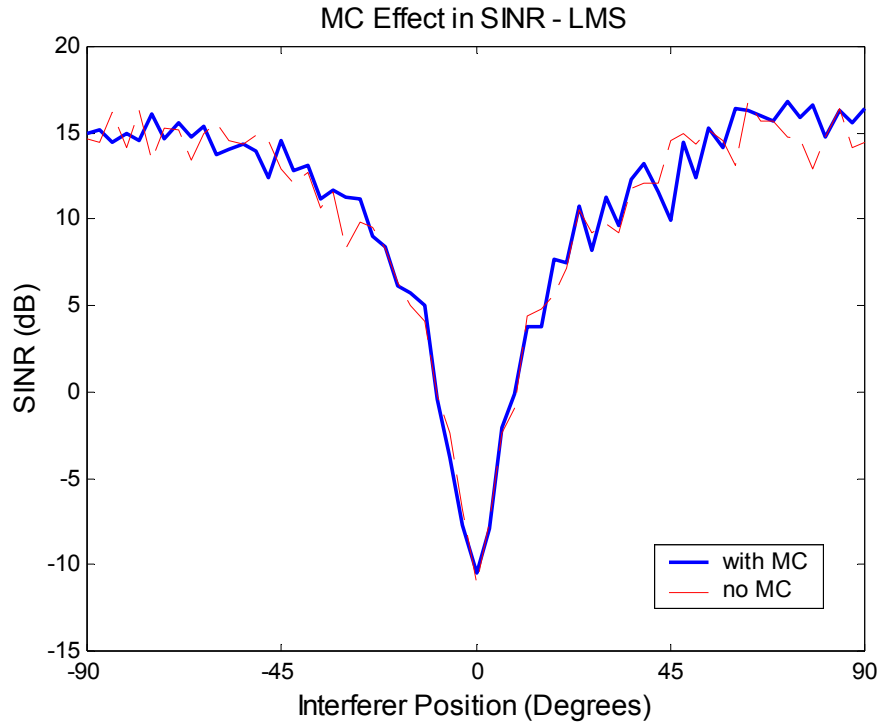

Figure 5.18 SINR pattern with respect to Θ_u − LMS ($\Theta_d = 0^o$, SNR=20dB, INR=20dB)

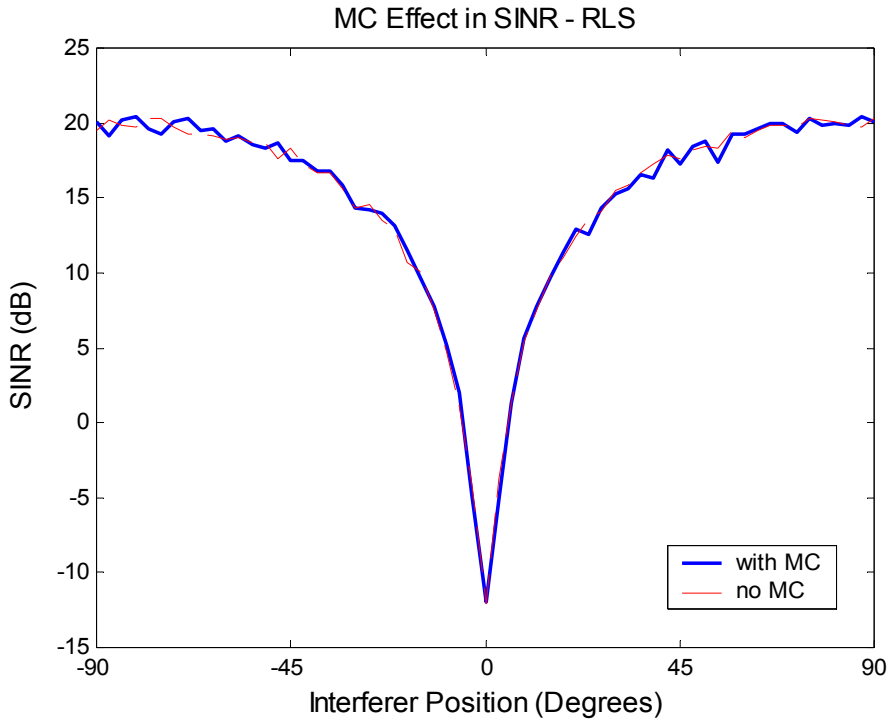

Figure 5.19 SINR pattern with respect to Θ_u − RLS ($\Theta_d = 0^o$, SNR=20dB, INR=20dB)

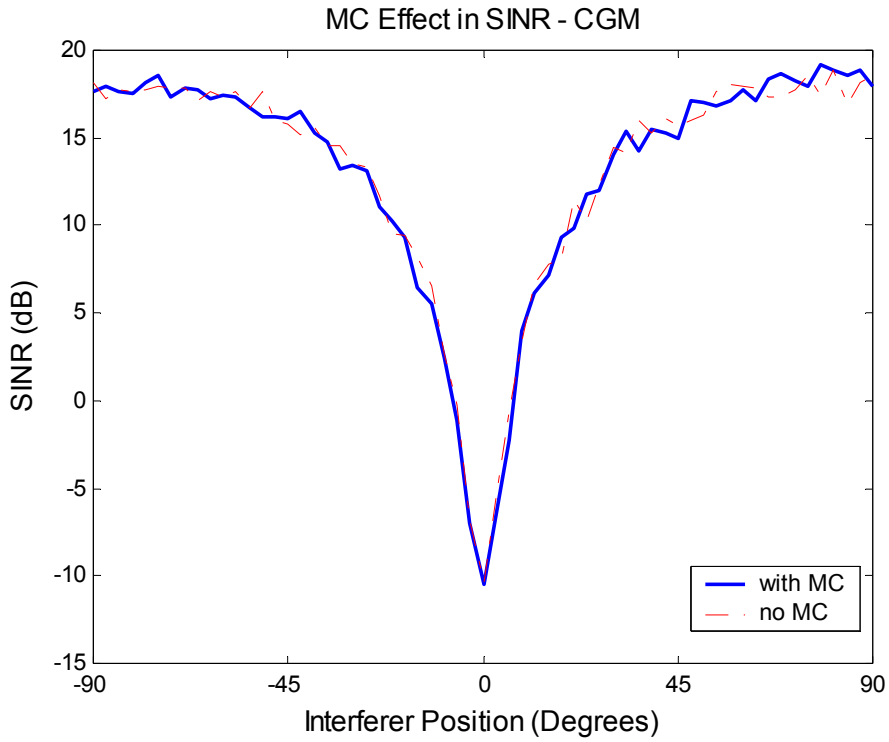

Figure 5.20 SINR pattern with respect to Θ_u – CGM ($\Theta_d = 0^o$, SNR=20dB, INR=20dB)

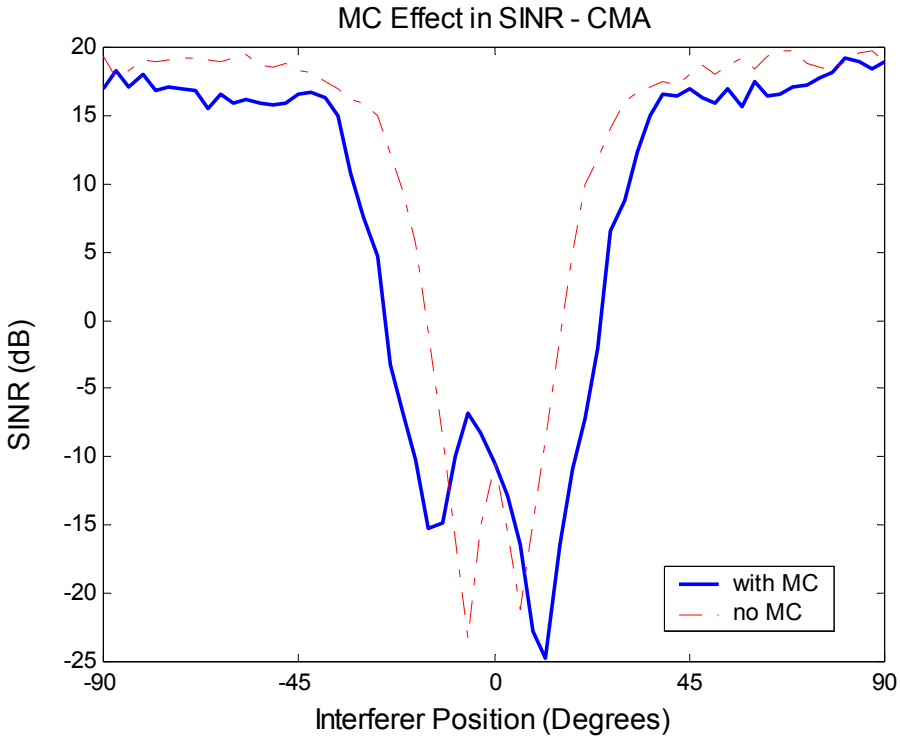

Figure 5.21 SINR pattern with respect to Θ_u – CMA ($\Theta_d = 0^o$, SNR=20dB, INR=20dB)

CHAPTER 6

CONCLUSIONS

In this thesis the effects of mutual coupling between the antenna elements on the performance of adaptive arrays are investigated. Three non-blind and one blind adaptive algorithms are selected for comparison. First, the interference suppression capability of least mean squares (LMS), recursive least squares (RLS), conjugate gradient method (CGM) and constant modulus algorithms (CMA) are investigated and it is observed that all of the algorithms generate similar radiation patterns which maximize the desired signal power and minimize the interference when the interference to noise ratio is greater than the desired signal to noise ratio. As the interferer power drops below the signal power, the depth of the null formed towards the interferer gets shallower which indicates that the algorithms have the precedence of maximizing the desired signal.

The convergence of weights for the adaptive algorithms are compared and the results of speed of convergence are tabulated using the ensemble averaged-squared error values for different iteration sets. Consequently, it is observed that the CGM is the most accurate and the LMS is the least accurate of the non-blind algorithms. When the speed of convergence is considered, the RLS is the slowest where the CGM is the fastest. It is hard to keep the envelope of the received signal in a CMA array. Therefore the blind algorithm CMA is the worst in accuracy and speed when compared with the non-blind algorithms.

It is also stated that the effect of mutual coupling on the performance of the non-blind algorithms is negligible. No matter how high the degree of mutual coupling, these algorithms obtain appropriate weight sets to achieve optimal solution using the reference signal. However, the performance of the CMA is affected severly with mutual coupling since the received signal deviates from constant amplitude property. It becomes harder to obtain a proper weight set for CMA. Consequently, the accuracy in CMA is poorer and the mutual coupling undermines the performance of CMA considerably.

Comparing the SINR performances, it is clearly observed that the mutual coupling does not effect the SINR performance of non-blind algorithms considerably. But the performance is far more degraded in CMA with mutual coupling. It can be stated that the scattering parameters of an adaptive antenna array using CMA technique should be measured carefully when handling an adaptive process in order not to be affected by mutual coupling between the antenna elements.

REFERENCES

[1] IEEE Trans. Antennas Propagat. (Special Issue on Active and Adaptive Antennas), vol. AP-12, Mar. 1964.

[2] D. L. Margerum, "Self Phased Arrays", in Microwave Scanning Antennas, vol. 3, R.C. Hansen, Ed. New York: Academic Press, 1966, ch. 5

[3] P. W. Howells, "Intermediate frequency side-lobe canceller," U.S. Patent 3 202 990, Aug. 24 1965 (filled May 4, 1959).

[4] B. Widrow, "Adaptive filters I:Fundamentals," Stanford Univ. Electronics Lab., Syst. Theory Lab., Center for Syst. Res., Rep. SU-SEL-66-126, Tech. Rep. 6764-6, Dec. 1966.

[5] B. Widrow, "Adaptive filters," in Aspects of Network and System Theory, R. E. Kalman and N. DeClaris, Eds. NewYork: Holt, Reinhart and Winston, 1971. ch5.

[6] Jack H.Winters, "Smart Antennas for Wireless Systems" AT&T Labs-Research, IEEE Personal Communications, Feb., 1998

[7] Lal C. Godara, "Applications of Antenna Arrays to Mobile Communications, Part II: Beam-forming and Direction-of-Arrival Cosiderations", Proceedings of the IEEE, vol. 85, No.8, August 1997, pp. 1198-1220

[8] Jack H.Winters, J. Salz, and R. D. Gitlin, "The Impact of Antenna Diversity on the Capacity of Wireless Communication Systems," IEEE Trans. Commun., vol. 42, pp. 1740-1751, 1994

[9] S. Choi, and T. K. Sarkar, "Adaptive Antenna Array Utilizing The Conjugate Gradient Method For Multipath Mobile Communication," Signal Process., vol. 29, pp. 319-333, 1992

[10] S. Choi, Application of the Conjugate Gradient Method for Optimum Array Processing, vol. V. Amsterdam, The Netherlands: Elsevier, 1991, ch. 16.

[11] Hao Yuan, Kazuhiro Hirasawa, The Mutual Coupling and Diffraction Effects on the Performance of a CMA Adaptive Array, IEEE Trans on Vehicular Technology, vol. 47, no. 3, August 1998

[12] T. Tanaka, R. Miura, I. Chiba, and Y. Karasawa, "An ASIC implementation Scheme to realize a beam space CMA adaptive Antenna Array," IEICE Trans. Commun., vol. E78-B, pp. 1467-1473, Nov. 1995

[13] I. Chiba, W. Chujo, and M. Fujise, "Beamspace Constant Modulus Algorithm Adaptive Array Antennas," in Proc. Inst. Elect. Eng. 8th Int. Conf. Antennas and Propagation, Edinburgh, Scotland, 1993, pp. 975–978.

[14] H. Steyskal, J. Herd, "Mutual Coupling in Small Array Antennas," IEEE Trans. On Antennas and Propagation, vol. 38, No.12, Dec 1990

[15] J. M. Cioffi and T. Kailath, "Fast recursive-least-square, transversal filters for adaptive filtering," IEEE Trans. Acoust., Speech, Signal Processing, vol. ASSP-32, pp. 998–1005, 1984.

[16] M. G. Larimore and J. R. Treichler, "Convergence behavior of the constant modulus algorithm," in Proc. ICASSP, Apr. 1983, pp. 13–16

[17] Raviraj S. Adve and Tapan Kumar Sarkar, "Compensation for the Effects of Mutual Coupling on Direct Data Domain Adaptive Algorithms" IEEE Trans. On Antennas and Propagation, vol. 48, No. 1, Jan 2000

[18] B.Friedlander and A.J.Weiss, "Direction Finding in the Presence of Mutual Coupling" IEEE Trans. On Antennas and Propagation, vol. 39, No. 3, Mar 1991

[19] S.Haykin "Communication Systems", John Wiley&Sons Inc.,Third Edition, 1995, pp.605-606